

Glitches in Southern Pulsars

N. Wang,^{1,2,3} R. N. Manchester,² R. T. Pace,^{2*} M. Bailes,⁴ V. M. Kaspi,^{5,6}

B. W. Stappers^{7†} and A. G. Lyne⁸

¹ Urumqi Astronomical Observatory, CAS, 40 South Beijing Road, Urumqi 830011, China; email:wangna@ms.xjb.ac.cn

² Australia Telescope National Facility, CSIRO, P.O. Box 76, Epping NSW 1710, Australia; email:rmanches@atnf.csiro.au

³ Geophysics Department, Peking University, Beijing 100871, China

⁴ Astrophysics and Supercomputing, Swinburne University of Technology, PO Box 218, Hawthorn, Vic. 3122, Australia

⁵ MIT, Center for Space Research 37-621, 70 Vassar St., Cambridge MA 02139, USA

⁶ McGill University, Physics Department, 3600 University Street, Montreal, Quebec, Canada H3A 2T8

⁷ Mt Stromlo Observatory, ANU, Private Bag, Weston Creek ACT 2611, Australia

⁸ University of Manchester, Nuffield Radio Astronomy Laboratories, Jodrell Bank, Macclesfield, Cheshire SK11 9DL, UK

27 October 2018

ABSTRACT

Timing observations of 40 mostly young pulsars using the ATNF Parkes radio telescope between 1990 January and 1998 December are reported. In total, 20 previously unreported glitches and ten other glitches were detected in 11 pulsars. These included 12 glitches in PSR J1341–6220, corresponding to a glitch rate of 1.5 glitches per year. We also detected the largest known glitch, in PSR J1614–5047, with $\Delta\nu_g/\nu \approx 6.5 \times 10^{-6}$ where $\nu = 1/P$ is the pulse frequency. Glitch parameters were determined both by extrapolating timing solutions to inter-glitch intervals and by phase-coherent timing fits across the glitch(es). These fits also gave improved positions and dispersion measures for many of the pulsars. Analysis of glitch parameters, both from this work and from previously published results, shows that most glitches have a fractional amplitude $\Delta\nu_g/\nu$ of between 10^{-8} and 10^{-6} . There is no consistent relationship between glitch amplitude and the time since the previous glitch or the time to the following glitch, either for the ensemble or for individual pulsars. As previously recognised, the largest glitch activity is seen in pulsars with ages of order 10^4 years, but for about 30 per cent of such pulsars, no glitches were detected in the 8-year data span. There is some evidence for a new type of timing irregularity in which there is a significant increase in pulse frequency over a few days, accompanied by a decrease in the magnitude of the slowdown rate. Fits of an exponential recovery to post-glitch data show that for most older pulsars, only a small fraction of the glitch decays. In some younger pulsars, a large fraction of the glitch decays, but in others, there is very little decay. Apart from the Crab pulsar, there is no clear dependence of recovery timescale on pulsar age.

Key words: stars: neutron – pulsars: general

1 INTRODUCTION

Timing observations have shown that pulsars are remarkably stable clocks (e.g. Kaspi, Taylor & Ryba 1994). However, they are not always predictable. Two types of instability have been observed. In the first, the pulsar period, P , or frequency $\nu = 1/P$, varies in an apparently random fashion, fluctuating on timescales of days, weeks, months and

years (Cordes & Downs 1985). The intensity of the fluctuations can be described by an ‘activity parameter’ based on the amplitude of the second frequency-derivative term in a Taylor-series fit to a set of pulse times of arrival (TOAs):

$$\Delta(t) = \log \left(\frac{|\ddot{\nu}|}{6\nu} t^3 \right) \quad (1)$$

where t is the length of the data span in seconds (Arzoumanian et al. 1994). Conventionally $t = 10^8$ s is adopted, giving the parameter Δ_8 . In most young pulsars, the magnitude of $\ddot{\nu}$ is far in excess of that expected from secular slowdown. Furthermore, timing noise is normally very ‘red’ (Cordes & Downs 1985) and so the second derivative term is a good in-

* Present Address: Department of Physics and Mathematical Physics, University of Adelaide, Adelaide SA 5005, Australia

† Present Address: Astronomical Institute, University of Amsterdam, Kruislaan 403, 1098 SJ Amsterdam, The Netherlands

indicator of the level of noise. Observations of large samples of pulsars (Cordes & Downs 1985; D’Amico et al. 1998) show that the activity parameter is positively correlated with the value of \dot{P} , the first time-derivative of the pulsar period.

In the second type of period instability, known as a ‘glitch’, the pulse frequency has a sudden increase which typically has a fractional amplitude $\Delta\nu_g/\nu$ in the range $10^{-8} - 10^{-6}$. These glitches are unpredictable but typically occur at intervals of a few years in young pulsars. Coincident with the glitch, there is often an increase in the magnitude of the frequency derivative, typically by ~ 1 per cent, which sometimes decays with a timescale of weeks to years. The time-dependence of the pulsar frequency after a glitch is generally well described by the following function:

$$\nu(t) = \nu_0(t) + \Delta\nu_g[1 - Q(1 - \exp(-t/\tau_d))] + \Delta\dot{\nu}_p t \quad (2)$$

where $\nu_0(t)$ is the value of ν extrapolated from before the glitch, $\Delta\nu_g = \Delta\nu_d + \Delta\nu_p$ is the total frequency change at the time of the glitch ($t = 0$), where $\Delta\nu_d$ is the part of the change which decays exponentially and $\Delta\nu_p$ is the permanent change in pulse frequency, $Q = \Delta\nu_d/\Delta\nu_g$, τ_d is the decay time constant and $\Delta\dot{\nu}_p$ is the permanent change in $\dot{\nu}$ at the time of the glitch. The increment in frequency derivative is given by

$$\Delta\dot{\nu}(t) = \Delta\dot{\nu}_d \exp(-t/\tau_d) + \Delta\dot{\nu}_p = \frac{-Q\Delta\nu_g}{\tau_d} \exp(-t/\tau_d) + \Delta\dot{\nu}_p. \quad (3)$$

The middle term of equation 2 was originally derived on the basis of the two-component model for glitch recovery (Baym et al. 1969), where the initial frequency jump was due to a ‘starquake’ or sudden change in moment of inertia of the solid crust. In this model, the parameter $Q = I_s/I_c$ where I_s and I_c are the moments of inertia of the superfluid component and the crust, respectively.

In later versions of the theory, the frequency jump is due to a sudden unpinning of vortex lines in crustal neutron superfluid (Anderson & Itoh 1975). Post-glitch relaxation may be due to ‘vortex creep’, that is, a slow drift of the vortices across the crustal lattice (e.g. Alpar, Cheng & Pines 1989) or drift of the crustal lattice itself with the vortices remaining pinned (Ruderman 1991; Ruderman, Zhu & Chen 1998).

Depending on the internal temperature of the star and other factors, the response to a glitch may be linear or non-linear (Alpar, Cheng & Pines 1989). In the linear regime, the frequency jump at $t = 0$ decays exponentially with time constant τ_d . The fractional change in frequency derivative at the jump is

$$\Delta\dot{\nu}_g/\dot{\nu} = (I_s/I)(\Delta\omega_s/\tau_d), \quad (4)$$

where $\Delta\omega_s$ is the change at the time of the glitch in the rotational lag of the superfluid, and $\omega_s = 2\pi(\nu_s - \nu)$, where ν_s is the rotation frequency of the neutron superfluid. For glitches which are large compared to the steady-state lag, $\Delta\omega_s \sim -2\pi\Delta\nu$ and the change in spin-down rate can be large compared to I_s/I .

In the non-linear regime, there is essentially no relaxation ($Q \approx 0$) and

$$\Delta\dot{\nu}_g/\dot{\nu} = I_s/I, \quad (5)$$

giving a permanent change $\Delta\dot{\nu}_p$ in $\dot{\nu}$ (Eqn 3). Analyses of data for the Vela pulsar and other pulsars (Alpar et al.

1988; Alpar et al. 1993; Ruderman, Zhu & Chen 1998) are generally consistent with a rather small superfluid fraction, $I_s/I \sim 10^{-2}$, participating in the glitch activity. In the Ruderman et al. (1998) model, permanent changes in $\dot{\nu}$ may result from a change in the magnetic field configuration associated with the crustal cracking at the time of a glitch.

Until the last few years, the number of known glitches and glitching pulsars was modest. However, with relatively high-frequency searches at low Galactic latitudes (Clifton et al. 1992; Johnston et al. 1992; Kaspi et al. 1992) discovering a much larger sample of young pulsars, the number has increased significantly, with 21 pulsars having 46 glitches being listed in the recent review by Lyne (1996). In this paper we describe timing observations of a sample of 40 mostly young pulsars using the Parkes radio telescope which show a total of 30 glitches in 11 pulsars.

2 OBSERVATIONS AND ANALYSIS

Observations were made using the Parkes 64-m radio telescope between 1990 January and 1998 December at frequencies around 430, 660, 1400 and 1650 MHz. The frequencies below 1 GHz were used only occasionally to improve the determination of dispersion measures (DMs). At all frequencies, cryogenic dual-channel receivers were used. Two separate back-end systems were used to provide the frequency resolution necessary for dedispersing. The early observations used filterbanks and a one-bit digitizer system constructed at Jodrell Bank; a $2 \times 256 \times 0.125$ MHz system was used at 430 MHz, a $2 \times 128 \times 0.25$ MHz system was used at 660 MHz and at the higher frequencies a $2 \times 64 \times 5$ MHz system was used. Further details of the filterbank data acquisition system may be found in Manchester et al. (1996). From 1994 July, data were acquired using a correlator system constructed at Caltech (Navarro 1994). This system used two-bit digitization and an autocorrelator with 2×256 lags over a maximum bandwidth of 128 MHz. From mid-1995, the lags were split between two frequency bands which gave simultaneous observations at radio frequencies of 1400 and 1650 MHz (Sandhu et al. 1997).

For the filterbank systems, data were folded synchronously with the pulsar period using off-line programs to give mean total intensity pulse profiles. In the correlator system this folding was performed in a hardware integrator having 1024 bins across the pulsar period. For both systems, integration start times were established to better than 1μ s using time signals from the Observatory clock system. This was related to UTC(NIST) using a radio link to the NASA DSN station at Tidbinbilla and clock offsets kindly provided by the Jet Propulsion Laboratory, Pasadena. In subsequent analysis, the data were summed to form 8 or 16 frequency subbands and time subintegrations of 60 or 90 s duration and stored on disk. These files were then summed in frequency and time using the best available period and DM information to form a single profile for each observation. This was then cross-correlated with a standard profile for the pulsar to give a pulse time of arrival (TOA).

A total of 40 pulsars were monitored during the program. The J2000 and B1950 names of these pulsars, their periods and characteristic ages, and the dates spanned by the observations are listed in Table 1. Depending on the strength

of the pulsar, observation times for each TOA were between 2 and 12 min. Observations were obtained at intervals of between 2 and 6 weeks for most of the pulsars in Table 1, with the known glitching pulsars being observed more frequently. The TOAs resulting from this program were analysed using version 11.3 of TEMPO[‡] which includes provision for fitting the glitch parameters given in Equation 2. The DE200 solar-system ephemeris (Standish 1990) was used to convert TOAs to the solar-system barycentre. The sixth and seventh columns of Table 1 give the rms value of the TOA uncertainty (dependent on the pulse period, pulse shape and signal/noise ratio) and the rms residual after fitting for just pulse frequency and its first derivative. For glitching pulsars, the largest glitch-free interval was used for this fit. These residuals are dominated by the effects of timing noise, and so they are an indication of its amplitude. An exception to this is PSR J1513-5908, which has significant frequency second and third derivatives due to secular slowdown (Kaspi et al. 1994); in this case, the fit giving σ_T included the first three frequency derivatives.

For several pulsars, the position and DM were measured with comparable or better precision than was previously available. Positions were obtained using the so-called ‘pre-whitening’ method (Kaspi et al. 1994). In this method, the position is fitted along with sufficiently many frequency-derivative terms and in some cases, glitch terms, to ‘absorb’ the timing noise and give an approximately Gaussian distribution of timing residuals. DMs were measured from short sections of data where there were multi-frequency observations. This ensures that contamination by long-term timing noise is not a problem and that error estimates are realistic.

For glitches where the amplitude of the glitch and the interval between the last pre-glitch observation and the first post-glitch observation are not too large, the epoch of the glitch can be determined by requiring that the pulse phase be continuous over the glitch. In this situation, TEMPO gives an estimate of the glitch parameters, including the epoch, and their uncertainty. Where post-glitch decay parameters are estimated, these refer to the long-term decay, typically with timescales of hundreds of days. The resolution of our observations is generally not sufficient to detect the more rapid post-glitch recoveries observed in some pulsars, for example, the Vela pulsar (Flanagan 1990; McCulloch et al. 1990).

For larger glitches where there may be one or more turns of phase in the residuals between the bounding observations, the glitch epoch is uncertain. Other glitch parameters are affected by this uncertainty. To estimate uncertainties in this case, the following procedure was adopted. The glitch epoch was taken to be halfway between the bounding observations, with an uncertainty of half their separation. The increments $\Delta\nu_g$ and $\Delta\dot{\nu}_g$ were then computed for an assumed glitch epoch t_g by extrapolating the pre- and post-glitch fits to t_g and taking differences. Uncertainties were similarly extrapolated and quadrature sums taken for the uncertainties in the increments. This was done separately for t_g at the two bounding epochs. The final error estimates were then the quadrature sum of the difference between the increments at

either end of the data gap and the larger of the uncertainties in the increments.

3 RESULTS

Table 2 lists parameters for the 11 pulsars for which glitches were detected. The pulsar J2000 positions and DMs used in or derived from the analysis are given. Uncertainties in the last digit quoted are given in parentheses. These and other quoted uncertainties from TEMPO fits are twice the formal rms error. Position fits were generally to the largest available data span not too strongly affected by post-glitch post-glitch recovery. As described above, the data spans used to determine the positions and their errors were ‘pre-whitened’ to eliminate the effects of period noise from the positions and their errors. The fifth and sixth columns give the data span used when fitting the position and the final rms timing residual. References for the position and DM are given in the final column.

A total of 30 glitches were observed in these 11 pulsars. Independent fits to the pre-glitch, inter-glitch and post-glitch timing data are given in Table 3. Except for short sections of data, the fits include a $\ddot{\nu}$ term. In every case, this term is dominated by recovery from a previous glitch; the $\ddot{\nu}$ from the long-term secular slow down is negligible by comparison. Higher-order frequency derivative terms were not fitted, so the rms residuals given in right-most column reflect the presence of random period irregularities, especially for longer data spans.

Glitch parameters are listed in Table 4. If marked by *, the glitch epoch is determined by requiring phase continuity across the glitch. The next two columns give the fractional steps in ν and $\dot{\nu}$ at the glitch determined by extrapolating the pre- and post-glitch solutions (Table 3) to the glitch epoch, with uncertainties determined as described in Section 2. Parameters in the remaining columns were determined using TEMPO to fit phases across the glitch.

Ten of these glitches have been previously reported: single glitches in PSR J0835-4510 (Flanagan 1996), PSR J1709-4428 (Johnston et al. 1995; Shemar & Lyne 1996), PSR J1731-4744 (D’Alessandro & McCulloch 1997) and PSR J1801-2451 (Lyne et al. 1996a), and three glitches in PSR J1341-6220 (Kaspi et al. 1992; Shemar & Lyne 1996) and PSR J1801-2306 (Kaspi et al. 1993; Shemar & Lyne 1996). We reanalyse these glitches for completeness and consistency with the results for the other pulsars.

In the following sections we discuss each pulsar in turn.

3.1 PSR J0835-4510, PSR B0833-45, the Vela pulsar

The Vela pulsar is well known to suffer many giant glitches (Cordes, Downs & Krause-Polstorff 1988; McCulloch et al. 1990; Lyne et al. 1996b) and is being regularly monitored at a number of observatories. At Parkes, we are unable to make such regular and frequent observations. In this paper, we describe observations of the latest glitch which has only been briefly reported (Flanagan 1996).

Table 3 gives the results of fitting for ν and its first two time derivatives, both before and after the glitch. The pre-glitch fit was obtained from an approximately 1-year

[‡] See <http://pulsar.princeton.edu/tempo/> for a description of TEMPO.

Table 1. Pulsars monitored for glitch activity

PSR J	PSR B	Period (s)	Age (ky)	MJD Range	σ_{TOA} (μ s)	σ_T (μ s)	Glitches detected
0536–7543	0538–75	1.2458	34937.0	48957–50827	396	7392	–
0742–2822	0740–28	0.1668	157.0	48932–51155	46	12777	–
0835–4510	0833–45	0.0893	11.3	50024–51155	23	39668	1
0908–4913	0906–49	0.1068	111.6	48957–51155	57	25992	–
0942–5552	0940–55	0.6644	462.9	48874–51137	153	107551	–
1001–5507	0959–54	1.4366	442.9	47913–51137	125	7802	–
1048–5832	1046–58	0.1237	20.4	47909–50940	49	99696	3
1057–5226	1055–52	0.1971	535.4	48814–51155	116	4569	–
1105–6107	–	0.0632	63.3	49176–51155	54	1176	2
1123–6259	–	0.2714	818.6	49316–51155	288	1329	1
1133–6250	1131–62	1.0229	35855.0	48928–51094	815	5814	–
1224–6407	1221–63	0.2165	692.2	47912–51155	39	1309	–
1320–5359	1317–53	0.2797	478.9	50536–51155	181	434	–
1326–5859	1323–58	0.4780	2358.5	50242–51094	72	2918	–
1328–4357	1325–43	0.5327	2796.0	50738–51155	190	228	–
1341–6220	–	0.1933	12.1	47915–51022	357	2309	12
1359–6038	1356–60	0.1275	318.7	50329–51155	18	102	–
1435–5954	–	0.4730	4857.5	49955–51135	413	2028	–
1453–6413	1449–64	0.1795	1035.0	50669–51093	13	87	–
1456–6843	1451–68	0.2634	42244.9	48330–51094	96	1175	–
1513–5908	1509–58	0.1502	1.5	48296–51155	241	2485	–
1539–5626	1535–56	0.2434	795.2	48874–51155	116	10560	–
1549–4848	–	0.2883	323.8	49574–51045	299	1749	–
1559–4438	1556–44	0.2571	3994.7	47910–51155	47	1728	–
1559–5545	1555–55	0.9572	740.5	49559–51135	277	36457	–
1602–5100	1558–50	0.8642	196.3	48297–51155	139	207783	–
1614–5047	1610–50	0.2316	7.4	48295–50926	148	19381	1
1637–4553	1634–45	0.1188	590.3	50669–51155	74	159	–
1644–4559	1641–45	0.4551	358.8	48956–51156	411	13055	–
1646–4346	1643–43	0.2316	32.5	47912–50502	350	162568	–
1709–4428	1706–44	0.1024	17.4	47909–51156	43	4862	1
1722–3712	1719–37	0.2362	345.9	49078–51094	58	10878	–
1730–3350	1727–33	0.1394	26.0	50538–51155	96	10344	–
1731–4744	1727–47	0.8297	80.3	49043–51156	62	8966	2
1739–2903	1736–29	0.3229	651.7	50739–51155	126	265	–
1752–2806	1749–28	0.5626	109.5	48145–51138	49	15282	–
1801–2304	1758–23	0.4158	58.3	48296–51156	561	5140	4
1801–2451	1757–24	0.1249	15.4	48896–50884	100	40947	2
1803–2137	1800–21	0.1336	15.8	50669–51155	123	1603	1
1822–4209	–	0.4565	15770.5	49540–51138	431	1801	–

data span and shows a significant $\dot{\nu}$ resulting from previous glitches. The post-glitch fit given in Table 3 is for an 82-day span commencing 18 days after the glitch. A timing model with polynomial terms up to $\dot{\nu}$ is not a good fit to longer data spans.

Fig. 1 shows the time dependence of the frequency residual $\Delta\nu$ and of $\dot{\nu}$ around the time of the glitch. The $\Delta\nu$ values plotted are differences between the values of ν obtained from independent fits to short sections of data, typically of span 20 – 30 days, and those determined from the predictions of the pre-glitch model given in Table 3. This plot shows an approximately exponential recovery in $\dot{\nu}$ after the glitch, followed by an approximately linear increase in $\dot{\nu}$. This be-

haviour is similar to that seen in previous Vela glitches (Lyne et al. 1996b).

Flanagan (1997) gives $\Delta\nu_g/\nu = 2.15(2) \times 10^{-6}$ and an epoch for the glitch of 1996, October 13.394 UT, corresponding to MJD 50369.394. Fractional changes in ν and $\dot{\nu}$ at the time of the glitch, obtained by extrapolating the pre-glitch and post-glitch fits (Table 3) to the glitch epoch are given in the fifth and sixth columns of Table 4. Results of fitting the exponential model (Equation 2) to the interval from 350 days before the glitch to 200 days after are also given in Table 4. In this fit, ν , $\dot{\nu}$ and $\ddot{\nu}$ were held at their pre-glitch values (Table 3). The small rms residual shows that the exponential model with about 40 per cent of the initial glitch in frequency decaying on a timescale of about 900 d is a

Table 2. Parameters for glitching pulsars

PSR J	R.A.(J2000) (h m s)	Dec.(J2000) ($^{\circ}$ ' ")	DM (cm^{-3} pc)	MJD Range	σ_W (μs)	Ref. ^a Posn,DM
0835–4510	08:35:20.68(2) ^b	–45:10:35.8(3) ^b	68.094(4)	–	–	1,5
1048–5832	10:48:12.2(1)	–58:32:05.8(8)	129.10(1)	49043–50536	1150	5,1
1105–6107	11:05:26.17(4)	–61:07:51.4(3)	271.01(4)	49176–50402	1080	5,2
1123–6259	11:23:55.549(12)	–62:59:10.74(9)	223.26(3)	49708–51155	785	5,3
1341–6220	13:41:42.63(8)	–62:20:20.7(5)	717.3(6)	48874–49888	–	5,5
1614–5047	16:14:11.29(3)	–50:48:03.5(5)	582.8(3)	50269–50778	736	5,1
1709–4428	17:09:42.728(2)	–44:29:08.24(6)	75.69(5)	48928–51156	211	5,1
1731–4744	17:31:42.103(5)	–47:44:34.56(14)	123.33(2)	49415–50704	351	5,5
1801–2304	18:01:19.829(9)	–23:04:44.2(2)	1074(6)	–	–	4,1
1801–2451	18:01:00.223(7)	–24:51:27.1(1)	289(1)	–	–	1,1
1803–2137	18:03:51.35(3)	–21:37:07.2(5)	233.9(3)	–	–	1,1

^a Reference: 1. Taylor, Manchester & Lyne (1993) ; 2. Kaspi et al. (1996) ; 3. D’Amico et al. (1997) ; 4. Frail, Kulkarni & Vasisht (1993) ; 5. This paper.

^b Position is for epoch MJD 41380 with proper motion $\mu_{\alpha} = -48 \text{ mas yr}^{-1}$, $\mu_{\delta} = 35 \text{ mas yr}^{-1}$

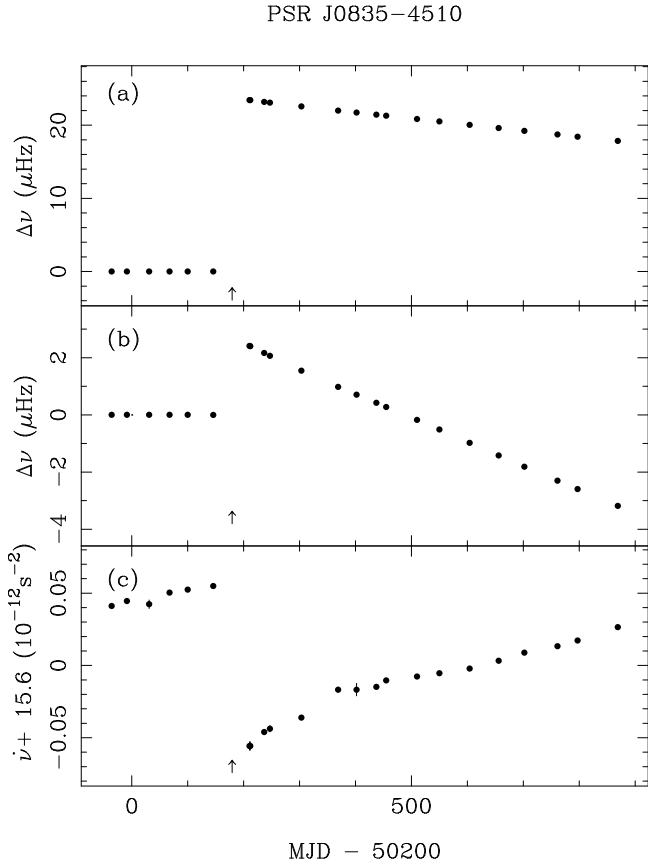


Figure 1. The 1996 October glitch of PSR J0835–4510: variations of (a) frequency residual $\Delta\nu$ relative to the pre-glitch solution, (b) an expanded plot of $\Delta\nu$ where the mean post-glitch value has been subtracted from the post-glitch data, and (c) the variations of $\dot{\nu}$. The epoch of the glitch is indicated by a small arrow near the base of each plot.

very good representation of the post-glitch relaxation, at least over the data span fitted. Fitting of ν , $\dot{\nu}$ and $\ddot{\nu}$ to the post-glitch data instead of the three parameters of the exponential fit gives a substantially worse fit with rms residual

360 μs and a systematic quartic term in the residuals. For the exponential fit, most of the rms residual comes from the first few post-glitch points which are positive, indicating an additional short-term recovery. However, it was not possible to fit for the parameters of this. The fitted glitch epoch, given in the third column of Table 4, is slightly earlier than that given by Flanagan (1997); this is consistent with the presence of more rapid post-glitch relaxation than modelled.

3.2 PSR J1048–5832, PSR B1046–58

This young pulsar was discovered in a high-frequency survey of the southern Galactic plane (Johnston et al. 1992). Evidence for gamma-ray pulsations has been found by Kaspi et al. (2000). The pulsar suffered two large glitches within the observed data span, the first of size $\Delta\nu_g/\nu \sim 3 \times 10^{-6}$ in 1993 February (MJD ~ 49034) and the second of size $\sim 0.7 \times 10^{-6}$ in 1997 December (MJD ~ 50788). Observed frequency residuals are shown in Fig. 2. The expanded plot of $\Delta\nu$ (Panel b) shows a third and much smaller glitch about 100 d before the large first glitch. Fits to the inter-glitch intervals (Table 3) give evidence for large fluctuations in the period. Fig. 3 gives timing residuals for the data span following the largest glitch, showing quasi-random fluctuations with a timescale of a few hundred days.

Table 2 gives an improved position for PSR J1048–5832 derived from the data following the largest glitch. Most of the systematic oscillation was removed by fitting up to the twelfth pulse frequency derivative at the same time as the position was determined. A fit to the whole data set, including parameters for the glitches, gave the same position within the combined errors. This position differs by $8''$ from that given by Johnston et al. (1995); this difference can be attributed to the different sets and the presence of the strong period irregularities. Recently, Stappers et al. (1999) have used the Australia Telescope Compact Array to determine an interferometric position for the pulsar: R.A. (J2000) $10^{\text{h}} 48^{\text{m}} 12^{\text{s}}.604 \pm 0^{\text{s}}.008$, Dec. (J2000) $-58^{\circ} 32' 03''.75 \pm 0''.05$. This position agrees with the timing position in R.A., but differs by $2''.45 \pm 0''.80$ in declination, probably as a result

Table 3. Pulse frequency parameters for glitching pulsars

PSR J	Int.	ν (s ⁻¹)	$\dot{\nu}$ (10 ⁻¹² s ⁻²)	$\ddot{\nu}$ (10 ⁻²⁴ s ⁻³)	Epoch (MJD)	Span (MJD)	No. of TOAs	Residual (μ s)
0835–4510	–1	11.1964839822(3)	–15.58140(4)	873(10)	50155.00	50024–50364	38	240
	1–	11.1955738808(10)	–15.61780(6)	985(12)	50847.00	50387–51155	223	3190
1048–5832	–1	8.087302320(3)	–6.27373(7)	72(10)	48419.00	47909–48929	59	10120
	1–2	8.0869925648(4)	–6.2719(4)	–	48991.00	48957–49026	9	113
	2–3	8.0865824929(8)	–6.28460(3)	146.7(14)	49790.00	49043–50786	164	21400
	3–	8.08599240181(15)	–6.29765(7)	390(40)	50889.00	50791–50940	51	190
1105–6107	–1	15.8248916396(18)	–3.95819(5)	–49(5)	49789.00	49176–50402	127	6426
	1–2	15.8246473365(3)	–3.96313(15)	–	50516.00	50433–50599	27	172
	2–	15.8245521708(20)	–3.96325(10)	–54(18)	50794.00	50433–51155	94	4306
1123–6259	–1	3.68413905495(20)	–0.07125(5)	–	49510.00	49316–49704	15	998
	1–	3.68413613509(3)	–0.0712993(10)	–	50432.00	49708–51155	195	817
1341–6220	–1	5.173922035(4)	–6.7727	–	47942.00	47915–47969	9	1402
	1–2	5.1737636204(9)	–6.77427(7)	–26(19)	48226.00	48011–48442	30	1778
	2–3	5.1735752982(4)	–6.7714(3)	–	48548.00	48465–48631	16	676
	3–4	5.1733890567(14)	–6.77215(7)	190(30)	48875.00	48635–49114	26	2309
	4–5	5.1732030931(11)	–6.7716(11)	–	49193.00	49159–49227	8	418
	5–6	5.173030116(14)	–6.767	–	49490.00	49488–49491	2	–
	6–7	5.1729425780(5)	–6.7677(3)	–	49640.00	49540–49739	9	678
	7–8	5.1728338894(5)	–6.7659(3)	–	49826.00	49762–49889	13	411
	8–9	5.172758037(3)	–6.753(3)	–	49956.00	49920–49993	12	1385
	9–10	5.1726390106(3)	–6.77150(3)	270(12)	50174.00	50025–50323	31	395
	10–11	5.1724946720(3)	–6.77004(6)	240(50)	50421.00	50341–50501	19	191
	11–12	5.1723883167(8)	–6.76847(19)	830(180)	50603.00	50536–50671	29	482
12–	5.1722422270(5)	–6.77115(7)	–10(19)	50859.00	50696–51022	83	1102	
1614–5047	–1	4.317954008(15)	–9.1886(3)	–523(143)	48409.00	48295–48523	32	2054
	–1	4.3177762511(8)	–9.1652(4)	–1905(670)	48633.00	48596–48669	11	172
	–1	4.3175461311(4)	–9.19054(4)	–73(12)	48923.00	48732–49114	23	820
	–1	4.317231719(4)	–9.1456(7)	–211(227)	49320.00	49159–49482	18	5104
	–1	4.3169526367(20)	–9.1552(4)	280(180)	49673.00	49559–49787	22	2549
	1–	4.3167356028(6)	–9.23644(4)	350(30)	49981.00	49818–50143	52	1001
	1–	4.3163251092(3)	–9.225923(13)	–204(3)	50496.00	50214–50777	87	1239
	1–	4.3160405830(14)	–9.2199(3)	–1600(300)	50853.00	50780–50926	34	1132
1709–4428	–1	9.7612713776(3)	–8.863749(8)	124.1(14)	48328.00	47909–48746	44	559
	1–	9.7608645977(8)	–8.89001(13)	181(14)	48885.00	48812–48959	21	183
	1–	9.7599781350(7)	–8.857444(12)	173.1(7)	50042.00	49000–51156	238	9857
1731–4744	–1	1.20510332177(3)	–0.237549(7)	–	49204.00	49043–49364	24	375
	1–2	1.20508592522(8)	–0.237668(3)	2.5(3)	50059.00	49415–50703	94	3403
	2–	1.20506786194(6)	–0.237616(5)	5.6(13)	50939.00	50722–51156	47	565
1801–2304	–1	2.4051602072(9)	–0.6527(6)	–	48357.00	48296–48417	11	1451
	1–2	2.40512168588(17)	–0.653540(5)	2.7(6)	49054.00	48464–49644	58	2961
	2–3	2.40507531889(14)	–0.65347(5)	–	49878.00	49730–50027	27	1107
	3–4	2.40505493478(18)	–0.65346(7)	–	50240.00	50116–50364	23	1018
	4–	2.4050229993(3)	–0.652923(12)	47(3)	50809.00	50461–51156	100	3246
1801–2451	–1	8.007176212(3)	–8.17639(11)	130(40)	49141.00	48896–49387	21	2256
	1–2	8.0065388371(19)	–8.19045(7)	399(7)	50064.00	49481–50647	89	12262
	2–	8.0060495257(7)	–8.20337(10)	–140(60)	50770.00	50656–50884	64	669
1803–2137	–1	7.4832982197(3)	–7.4889(3)	–	50710.00	50669–50751	16	176
	1–2	7.4832434845(19)	–7.5440(6)	4500(700)	50831.00	50779–50883	13	588
	2–	7.4831211339(4)	–7.52780(5)	484(190)	51019.00	50883–51156	10	152

Table 4. Glitch parameters for eleven pulsars

PSR J	Glt. No.	Glitch Epoch (Date) (MJD)		Extrapolated				Fitted		Resid. (μ s)
				$\Delta\nu_g/\nu$ (10^{-9})	$\Delta\dot{\nu}_g/\dot{\nu}$ (10^{-3})	$\Delta\nu_g/\nu$ (10^{-9})	$\Delta\dot{\nu}_g/\dot{\nu}$ (10^{-3})	Q	τ_d (d)	
0835–4510	1	961013	50369.345(2)*	2110(17)	5.95(3)	2132(52)	–	0.38(2)	916(48)	242
1048–5832	1	921118	48944(2)*	25(2)	0.3(1)	19(2)	–	–	–	865
	2	930216	49034(9)	2995(7)	3.7(1)	3000(10)	–	0.025(3)	100	1630
	3	971206	50788(3)	771(2)	4.62(6)	769(3)	–	0.245(3)	400	465
1105–6107	1	961130	50417(16)	281(3)	1.3(2.9)	279.7(2)	4.63(4)	–	–	480
	2	970613	50610(3)*	1.3(2)	0.19(1)	2.1(3)	–	–	–	420
1123–6259	1	941219	49705.87(1)*	749.12(12)	1.0(4)	749.31(14)	–	0.0026(1)	840(100)	848
1341–6220	1	900408	47989(21)	1507(1)	0.15(6)	1509(1)	–	–	–	2352
	2	910716	48453(12)	24.2(9)	0.50(7)	22.5(7)	–0.51(5)	–	–	–
	3	920124	48645(10)	990(3)	0.7(1)	996(3)	–	0.020(3)	75	–
	4	930527	49134(22)	10(2)	0.6(2)	13.2(13)	–	–	–	–
	5	940111	49363(130)	142(21)	0.68(16)	146(38)	–	–	–	–
	6	940620	49523(17)*	33(3)	–0.55(9)	37(35)	–	–	–	–
	7	950218	49766(2)*	11(1)	–0.26(6)	15(2)	–	–	–	–
	8	950706	49904(16)	16(7)	–1.9(4)	31(1)	–	–	–	–
	9	951018	50008(16)	1636(13)	3.3(4)	1648(3)	–	0.004(1)	300	–
	10	960826	50321.7(6)*	27(1)	0.61(6)	29.9(8)	–	–	–	–
	11	970322	50528.9(8)*	20(4)	1.0(4)	23.4(5)	–	–	–	–
	12	970823	50683(13)	703(4)	1.2(3)	707.5(7)	–	–	–	–
1614–5047	1	950326	49803(16)	6456(56)	9.7(2)	6460(80)	–	0.538(11)	2000	2168
1709–4428	1	920605	48778(34)	2012.3(2)	0.20(6)	2028(20)	–	0.133(7)	1420(90)	16670
1731–4744	1	940204	49387.3(2)*	135(1)	1.11(8)	139.2(6)	–	0.079(3)	263(23)	1171
	2	970912	50703(5)*	2.6(6)	0.8(1)	3.1(5)	–	0.25(13)	250	–
1801–2304	1	910717	48454.1(3)*	346(7)	1.5(9)	351(1)	–	–	–	5061
	2	941213	49701(1)*	64.7(5)	0.18(7)	60.8(4)	–	–	–	–
	3	951205	50050(5)*	22.6(6)	0.02(14)	17.0(5)	–	–	–	–
	4	961125	50392(70)	84(6)	1.7(8)	87(2)	–	0.25(3)	100	–
1801–2451	1	940504	49476(6)	1998(7)	4.85(28)	1988(34)	–	0.188(12)	800(60)	5023
	2	970722	50651(5)	1237(4)	3.87(9)	1248(9)	–	0.202(6)	600	–
1803–2137	1	971104	50765(15)	3200(27)	10.7(15)	3185(25)	–	0.161(6)	855(35)	334
	2	971104	50765(15)	–	–	27(3)	–	0.010(3)	18(2)	–

* Glitch epoch determined by phase fit.

of unmodelled period irregularities affecting the timing position.

Extrapolation of fits to the data sets on either side of the glitches gives the estimates of glitch parameters listed in columns 5 and 6 of Table 4. Glitch parameters from TOA fits are given in the remaining columns. Because of the contaminating effect of the period fluctuations, the parameters of the large glitches were determined by fitting the data span 100 – 150 days before and after each glitch. The effects of the earlier small glitch were determined separately by fitting the interval between 80 days prior to it and up to the large glitch, and were subtracted from the fit to the large glitch. Parameters from these fits are given in Table 4. Because of the large systematic period variations, it is not possible to reliably measure the post-glitch decay times. Fig. 3 gives some evidence for a relaxation with a timescale of ~ 100 d

following the 1993 glitch and somewhat longer for the 1997 glitch. Setting the decay time to 100 d and 400 d respectively for these two glitches gave the parameters listed in Table 4. The derived Q for the 1997 glitch appears significantly larger than that for the 1993 glitch, but this result is uncertain given the uncertainty in the relaxation time and the short data span following the glitch.

3.3 PSR J1105–6107

PSR J1105–6107 is a young pulsar with the relatively short period of 63 ms discovered in 1993 using the Parkes radio telescope (Kaspi et al. 1997). It is located close to but outside the boundaries of the supernova remnant G290.1–0.8 and within the error box for the EGRET gamma-ray source 2EG J1103–6106 (Kaspi et al. 2000). Its association with

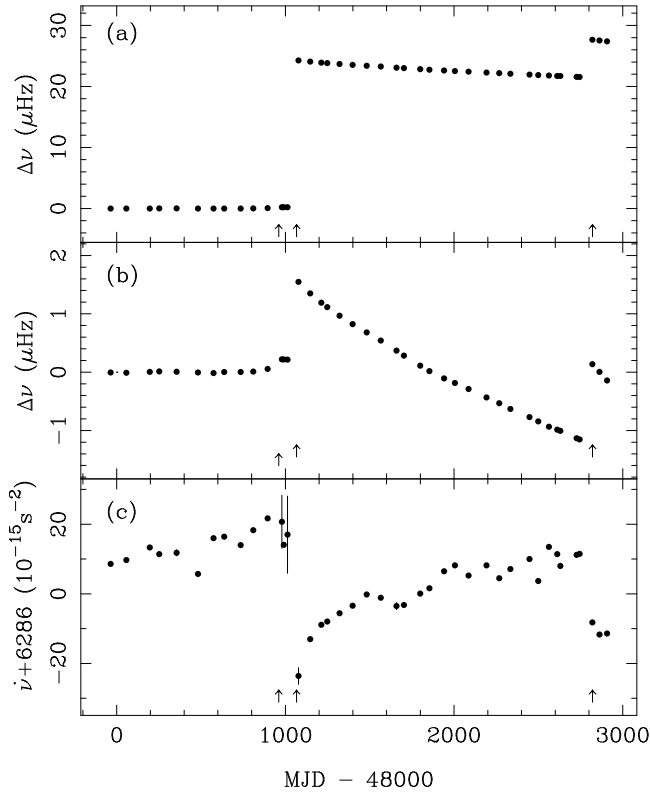


Figure 2. Glitches of PSR J1048–5832: variations of (a) frequency residual $\Delta\nu$ relative to the pre-glitch solution, (b) an expanded plot of $\Delta\nu$ where, for the second and third glitches, the mean residual up to the next glitch, or to the end of the data if there is no following glitch, has been removed from the corresponding interval (indicated by the raised arrows), and (c) the variations of $\dot{\nu}$.

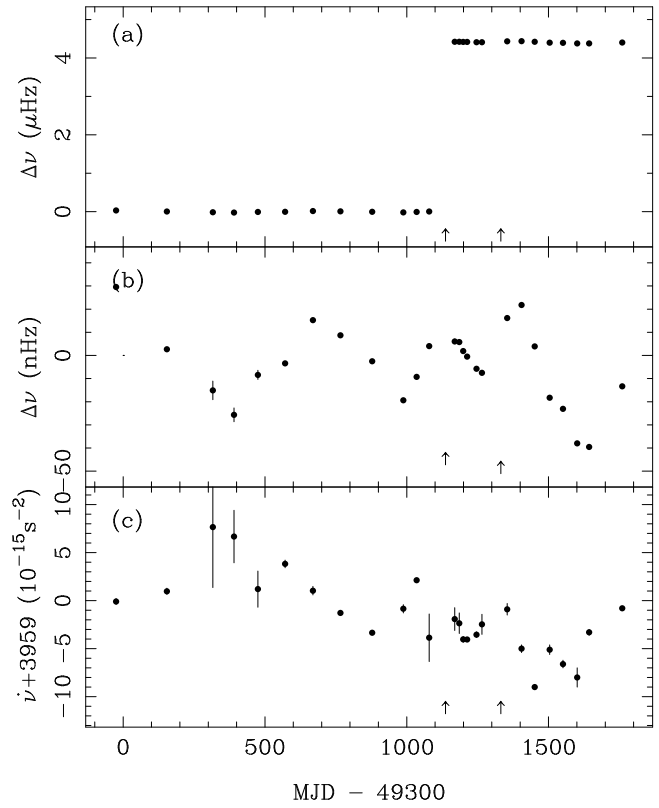


Figure 4. Glitches of PSR J1105–6107: variations of (a) frequency residual $\Delta\nu$ relative to the pre-glitch solution, (b) an expanded plot of $\Delta\nu$ where the mean residual between the large glitch and the second glitch has been removed from the data following the large glitch (indicated by the raised arrow), and (c), the variations of $\dot{\nu}$.

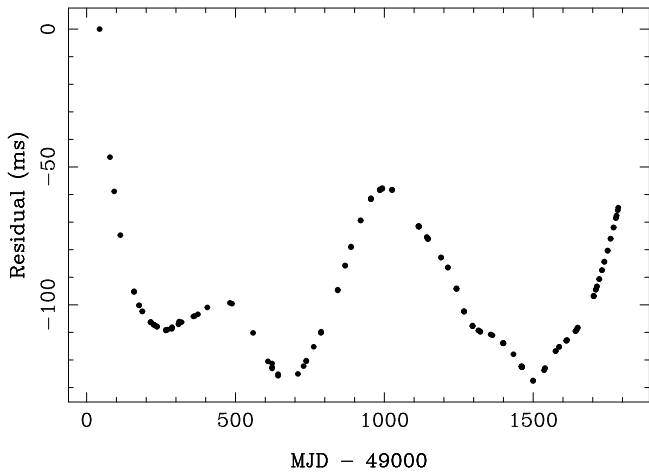


Figure 3. Timing residuals for PSR J1048–5832 between the two large glitches.

these objects remains plausible but unproven. Kaspi et al. (1997) reported on timing observations from 1993 July to 1996 July. Here we extend this interval to the end of 1998, and show that there were two glitches, a large one around the end of November, 1996 (MJD ~ 50417), and a small one about 200 days later.

Fig. 4 gives the variations in pulse frequency and frequency derivative over the observed data span, clearly showing the larger glitch which is of fractional size $\Delta\nu_g/\nu \sim 0.28 \times 10^{-6}$. There was a gap between bracketing observations of about 30 days, so the glitch epoch is not well determined. The expanded plot (b) shows that, despite the substantial period irregularities, there is good evidence for a small glitch about 200 days after the large glitch. Fig. 5 shows phase residuals around the time of this small glitch. Although this glitch is by far the smallest discussed in this paper, there is little doubt about its reality. Another small glitch may have occurred near the end of the data set, but there are insufficient post-glitch observations to confirm this. The position given in Table 2 was determined from a fit to the data prior to the large glitch, with seven frequency derivatives to absorb the period irregularities.

Table 3 gives fits to the three data spans delimited by the data set and the two glitches; the position was held at the value quoted in Table 2. The second derivative terms

PSR J1105–6107

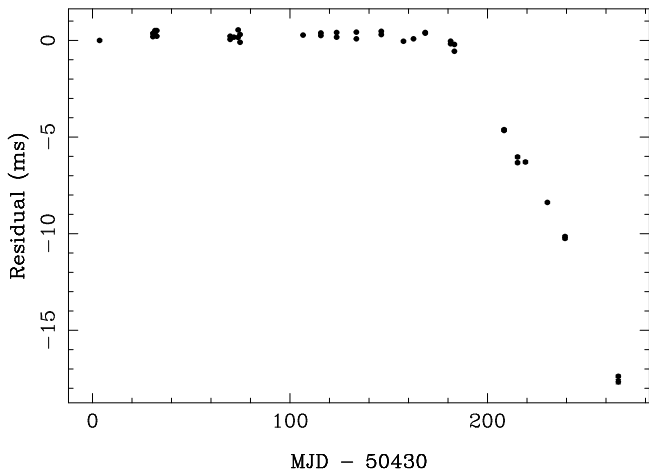


Figure 5. Timing residuals around the time of the small glitch in the period of PSR J1105–6107.

in the first and third fits are dominated by random period irregularities. Glitch parameters obtained by extrapolating these fits and from phase fits across the glitches are given in Table 4. Because of the period noise, the phase fits were restricted to intervals of 150 days before the first glitch, the inter-glitch interval, and 150 days after the second glitch. The fractional increase $\dot{\nu}$ after the first glitch is small, implying a similarly small value of the ratio Q/τ_d (Equation 3). Because of the small data span, τ_d is not well determined, but taking 100 d gives $Q \sim 0.035$; i.e., only a few percent of the glitch is likely to decay. This is confirmed by a fit to the whole data span including both glitches.

3.4 PSR J1123–6259

PSR J1123–6259, discovered in the Parkes southern pulsar survey (Manchester et al. 1996), has a period of 271 ms and a modest period derivative, giving a characteristic age of $\sim 8 \times 10^5$ yr. Despite this relatively large characteristic age, a glitch was detected between 1994 December 17–22 (MJD ~ 49706). The pulsar position was determined from the post-glitch data (Table 2); no pre-whitening was necessary as random period irregularities are small in this pulsar. Fits to the pre- and post-glitch data with this position are given in Table 3. Extrapolation of these fits to a central epoch (Table 4) shows that the glitch was of magnitude $\Delta\nu/\nu \sim 7.5 \times 10^{-7}$.[§]

As Table 4 and Fig. 6 show, there was a small but significant increase in $|\dot{\nu}|$ at the time of the glitch. A fit to the entire data span including glitch parameters but with the position and pre-glitch frequency parameters held to the values given in Table 2 and Table 3 is an excellent fit to the data and gives an unambiguous value for the epoch of the

[§] A glitch of this magnitude was reported by D’Amico et al. (1998) to have occurred at MJD 48650 ± 20 (1992 December). This epoch is in error. It was in fact the December 1994 glitch discussed in this paper.

PSR J1123–6259

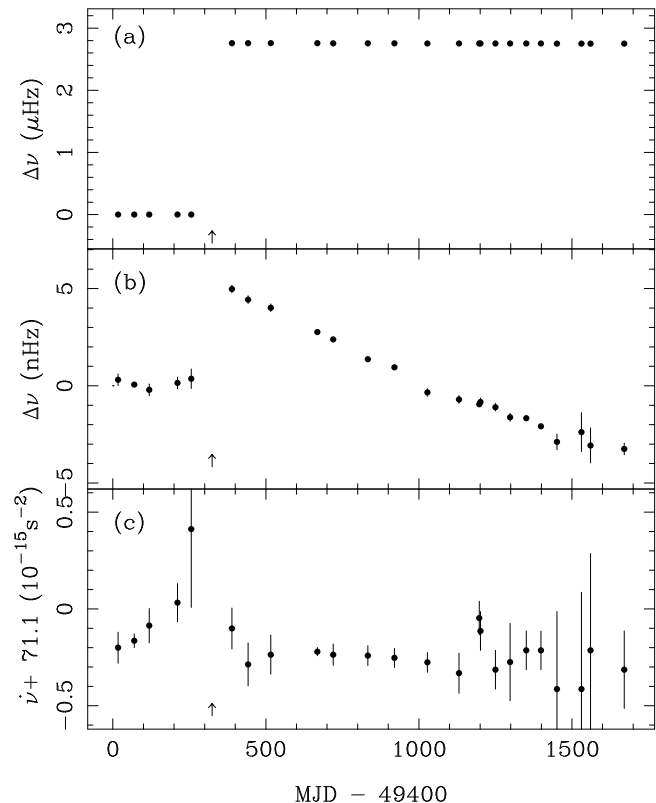


Figure 6. The 1994 December glitch of PSR J1123–6259: variations of (a) frequency residual $\Delta\nu$ relative to the pre-glitch solution, (b) an expanded plot of $\Delta\nu$ where the mean post-glitch value has been subtracted, and (c) the variations of $\dot{\nu}$.

glitch with an uncertainty of about 15 min on the assumption that there was phase continuity across the glitch. The derived value of Q is very small and the decay time is long (Table 4).

3.5 PSR J1341–6220

PSR J1341–6220 is a young pulsar (characteristic age $\sim 12,000$ y) discovered by Manchester et al. (1985) and associated with the supernova remnant G308–0.1 by Kaspi et al. (1992). Kaspi et al. reported two large glitches ($\Delta\nu_g/\nu \sim 1.5 \times 10^{-6}$ and $\sim 1.0 \times 10^{-6}$) and one smaller one ($\sim 2.3 \times 10^{-8}$) within the period 1990 January to 1992 May, making this one of the most actively glitching pulsars known. In this paper, we reanalyse the data from 1990 to 1992 and extend the data set 1998 March. Unfortunately, observations after this time were too sparse to permit unambiguous pulse counting.

The position given in Table 2 was determined in a simultaneous fit across the whole data set, including all glitches (see below). It has smaller estimated uncertainties than the position given by Kaspi et al. (1992), and lies $4''.3$ north of it. Given the prominence of period irregularities in this object, this difference, while twice the combined uncertainties, is of marginal significance. Determination of the DM is complicated by the strong scattering tail shown by this pulsar, even

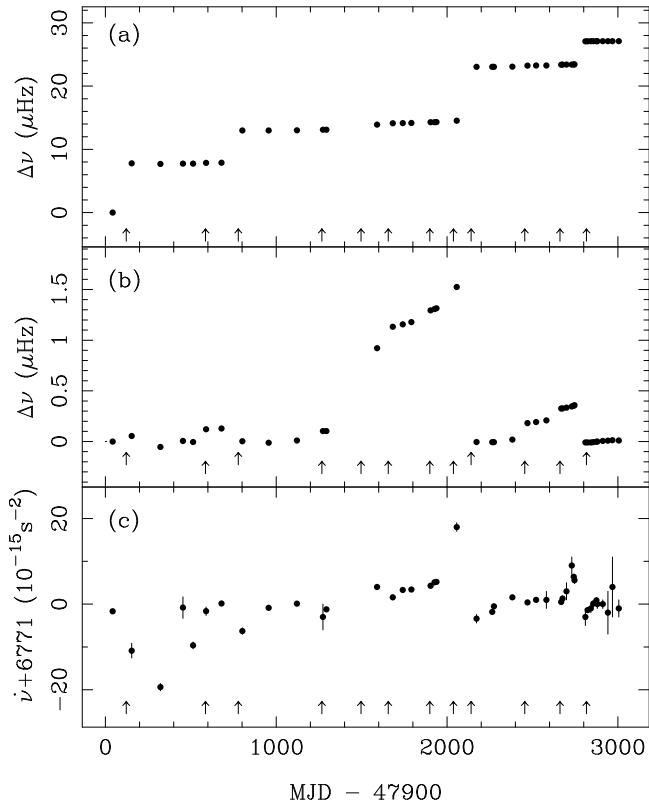


Figure 7. The glitches of PSR J1341–6220: variations of (a) frequency residual $\Delta\nu$ relative to the pre-glitch solution, (b) an expanded plot of $\Delta\nu$ where the mean residual between glitches with a raised arrow and the following glitch has been removed from data after the marked glitch, and (c) the variations of $\dot{\nu}$.

at frequencies around 1400 MHz. The value given in Table 2 was determined using TEMPO with data recorded between 1998 March and December at frequencies close to 1400 MHz and 1700 MHz. The relative phase of the standard profiles at the two frequencies was adjusted to allow for the effects of scattering. The derived DM is much more accurate than the value given by Kaspi et al. (1992) and just outside the error range of this value.

Fig. 7 shows the very complicated period history of this pulsar. A total of 12 glitches were observed in the 8.2-year interval, making this the most frequently glitching pulsar known, with a mean glitch interval of 250 days. The next most frequent is PSR B1737–30, with a mean interval of 345 days (Shemar & Lyne 1996). Four of the glitches were relatively large, with $\Delta\nu_g/\nu > 0.7 \times 10^{-6}$ and for two the fractional glitch size exceeds 10^{-6} . Most of the other glitches are quite small, with all except one having $\Delta\nu_g/\nu < 0.04 \times 10^{-6}$. They are, however, unambiguous on phase-time plots.

For most of the glitches, there is little evidence for any post-glitch relaxation. This is partly because of the relatively poorly sampled data, especially in the earlier years, but also because of the short time between successive glitches. For the third and ninth glitches, there is weak evidence in the $\dot{\nu}$ plot for some relaxation.

Table 3 gives fits to the inter-glitch intervals. Because of the limited data span prior to the first observed glitch, the

value of $\dot{\nu}$ was held fixed at a value close to the long-term mean for this fit. For about half of the intervals, there was a clear $\ddot{\nu}$ term in the residuals and this term was fitted.

Changes in ν and $\dot{\nu}$ at the time of each glitch, obtained by extrapolation of these fits to the glitch epoch, are given in Table 4. This table also gives glitch parameters from a single fit to the whole data set, solving simultaneously for the pulsar position, pulsar frequency (ν), mean frequency derivative ($\dot{\nu}$), and the parameters for all 12 glitches. As mentioned above, for most of the glitches, there was no significant post-glitch relaxation. For the third and ninth glitches, a post-glitch exponential decay was fitted; in both cases the decay time constant was not fitted for, but was determined by trial to minimise the final residual. In both cases the derived Q values are relatively small.

3.6 PSR J1614–5047, PSR B1610–50

This pulsar has a period of 231 ms and a very large period derivative (495×10^{-15}), implying a small characteristic age of ~ 7400 yr. In terms of its period irregularities, it is one of the noisiest pulsars known; this makes it difficult at times to keep track of the pulse phase. Since its discovery in late 1989 (Johnston et al. 1992), there has been no clear evidence for a glitch although, particularly where there is a significant gap in the timing data, it is often difficult to distinguish between a (small) glitch and more continuous period irregularities. However, in 1995 June (MJD ~ 49802), there was a massive glitch with $\Delta\nu_g/\nu \sim 6.5 \times 10^{-6}$, the largest ever observed in any pulsar (cf. Shemar & Lyne 1996). Fig. 8 shows this glitch and also illustrates the more continuous period irregularities.

These irregularities make it difficult to determine the pulsar position from timing data. Previously published positions have differed by much more than the quoted uncertainties (Taylor, Manchester & Lyne 1993; Johnston et al. 1995). Taking the data span from MJD 50269 to to 50778 (which is free of major irregularities – see below) and fitting for position and two frequency derivatives gives the position quoted in Table 2. An independent fit to the MJD range 48732 – 49093 gave a position with uncertainty of about $2''$, consistent with the position from the longer data span. Subsequent fits were made keeping the position fixed at the Table 2 value. Stappers et al. (1999) have recently determined an interferometric position for this pulsar: R.A. (J2000) $16^{\text{h}} 14^{\text{m}} 11^{\text{s}}.55 \pm 0'.01$, Dec. (J2000) $-50^{\circ} 48' 01''.9 \pm 0'.1$. As for PSR J1048–5832, the differences most probably result from period irregularities affecting the timing position.

The slope of the post-glitch data in the top two plots indicates a large change in frequency derivative at the time of the glitch. Because of the strong irregularities in the period, the pre- and post-glitch fits given in Table 3 are restricted to intervals of less than 300 days. Extrapolation of those fits gives the glitch parameters in columns 5 and 6 of Table 4. Glitch parameters were also obtained from a single timing solution over the same interval as the pre- and post-glitch fits (MJD 49559 – 50117) and are given in columns 7 – 10 of Table 4. This fit did not converge well when fitting for the glitch decay time, so this was held fixed at 2000 d, a value representative of those obtained from the fitting. From the post-fit residuals, it is clear that there is also a more rapid decay of a portion of the glitch with a timescale of 10 – 20 days. There is good agreement between the two methods of

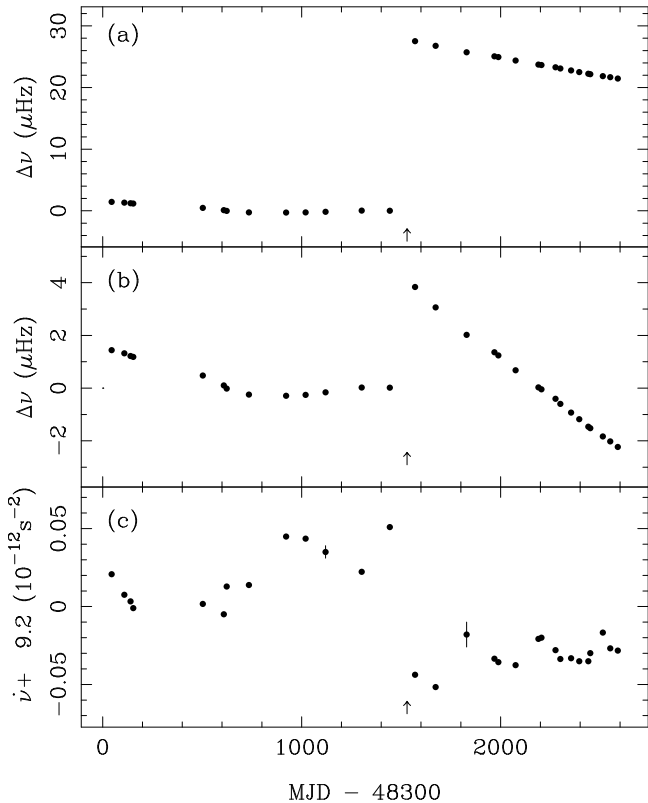


Figure 8. The 1995 June glitch of PSR J1614–5047: variations of (a) frequency residual $\Delta\nu$ relative to the pre-glitch solution, (b) an expanded plot of $\Delta\nu$ where the mean residual after the glitch has been removed, and (c) the variations of $\dot{\nu}$.

deriving the glitch parameters. From Equation 3, the Q and τ_d values given in Table 4 imply a fractional change in $\dot{\nu}$ of 0.0096, compared to 0.0097 from the extrapolation. Unfortunately, because of the large gap between the observations bracketing the glitch and the large size of the glitch, it is not possible to accurately determine the glitch epoch from phase continuity.

This is the largest glitch yet observed. The previous largest was for PSR B0355+54 for which $\Delta\nu/\nu$ was $\sim 4.37 \times 10^{-6}$ (Lyne 1987). There was very little decay of the frequency step in PSR B0355+54, whereas the Q value for the PSR J1614–5047 glitch indicates that more than half of it will decay away over a few years. In this respect, the PSR J1614–5047 glitch is more similar to the giant glitches in the Vela pulsar, which decay by a similar amount over similar timescales.

Phase fitting of post-glitch data revealed two further abrupt changes in pulse frequency. Phase plots for the intervals around these events are shown in Fig. 9. These phase plots have the character of glitch events, with a persistent fractional frequency change $\Delta\nu_g/\nu \sim 0.03 \times 10^{-6}$ at about MJD 50170 and 50780, respectively. The first event may indeed be a small glitch – it is not possible to tell because of the large data gap – but the second is not. This frequency change is resolved, taking place over about 10 days. In both cases, there appears to be a significant decrease in $|\dot{\nu}|$ asso-

ciated with the event. These rapid frequency changes could be classed as just part of the frequency irregularities which are prominent in this pulsar, but in general these irregularities have a much longer timescale and are smaller in amplitude. This is demonstrated by the small residuals for the fits to data before these events; for the second event, the fit includes only two frequency derivatives and has an rms residual of only 1.2 ms (Table 3). The MJD 50780 event stands out from the general irregularities with a much larger rate of frequency change over the 10 days. Phase fits to the post-glitch data given in Table 3 have been split into three sections to avoid contamination by these sudden frequency changes. The last ends at MJD 50926 (1998 April) since data are sparse after that point and it is not possible to fit across the gaps without ambiguity. The frequency second derivative terms are very significant in these fits, but differ greatly in both sign and magnitude for the different segments. They are clearly related to the period-noise processes occurring in this star and not to the secular slowdown.

3.7 PSR J1709–4428, PSR B1706–44

This pulsar, discovered by Johnston et al. (1992), is of interest for several reasons. It is young ($\tau_c \sim 17$ kyr) and has the third highest known value of \dot{E}/d^2 , where \dot{E} is the spin-down luminosity and d is the pulsar distance, after the Crab and Vela pulsars. It has been detected at gamma-ray wavelengths (Thompson et al. 1992; Thompson et al. 1996), X-ray wavelengths (Becker, Brazier & Trümper 1995) and possibly at TeV energies (Kifune et al. 1995). A supernova remnant association was proposed by McAdam, Osborne & Parkinson (1993), but deemed unlikely by Nicastro, Johnston & Koribalski (1996).

Johnston et al. (1995) presented results from two years of Parkes timing observations showing that the pulsar suffered a giant glitch of magnitude $\Delta\nu_g/\nu \sim 2 \times 10^{-6}$ near the end of May, 1992 (\sim MJD 48778). In this paper we analyse data from 1990 January to 1998 December. To determine the pulsar position, we have taken data from 150 days after the glitch (MJD 48928 – 51155) and fitted nine frequency derivatives to absorb the period irregularities. This fit had an rms residual of only 211 μ s and gave the position listed in Table 2. The derived position is about 12'' southeast of the position given by Johnston et al. (1995), but agrees better with an interferometric position given by Frail & Scharinghausen (1997): R.A. (J2000) $17^{\text{h}} 09^{\text{m}} 42^{\text{s}}.75 \pm 0^{\text{s}}.01$, Dec. (J2000) $-44^{\circ} 29' 06''.6 \pm 0''.3$. The timing fits described below were obtained with the position held at the Table 2 value.

Fig. 10 shows the large jump with a classic exponential recovery on a timescale of ~ 100 days coupled with a longer term relaxation. Fits of a cubic phase polynomial to the pre-glitch data, to the 150 days after the glitch and to data from 150 days post-glitch are given in Table 3. The post-glitch fit has large systematic residuals, dominated by the post-glitch recovery. Glitch parameters obtained by extrapolating the first and second fits to the glitch epoch are given in Table 4 along with those from a phase fit to the whole data set. This latter fit is strongly affected by the strong period irregularities (Fig. 11) and so the derived parameters are only approximate. There is clear evidence in the post-fit residuals for a more rapid exponential decay with time constant of the order of 100 days. However, it was not possible to fit

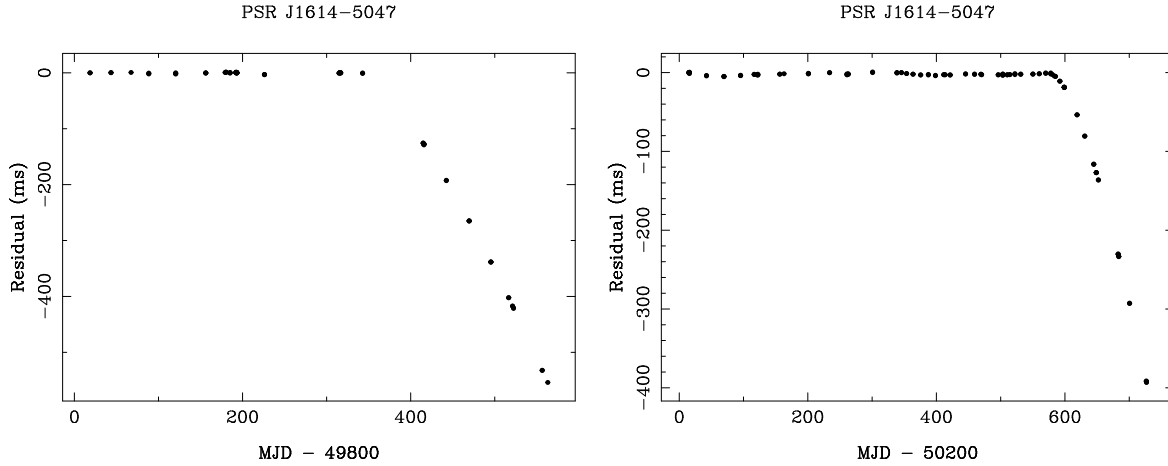


Figure 9. Variations of timing phase residuals around two epochs of rapid frequency change in PSR J1614–5047

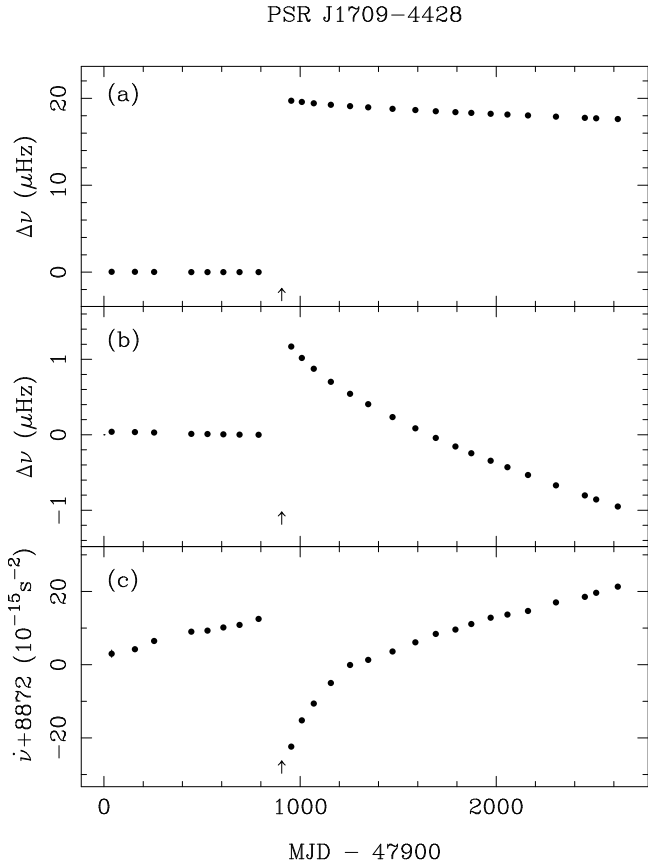


Figure 10. The 1992 May glitch (MJD 48778) of PSR J1709–4428: variations of (a) frequency residual $\Delta\nu$ relative to the pre-glitch solution, (b) an expanded plot of $\Delta\nu$ where the mean residual after the glitch has been removed, and (c) the variations of $\dot{\nu}$.

for the parameters of this owing to the contaminating effect of the period irregularities.

3.8 PSR J1731–4744, PSR B1727–47

PSR J1731–4744 is a long-period pulsar (0.830 s) which has a large period derivative giving a relatively low characteristic

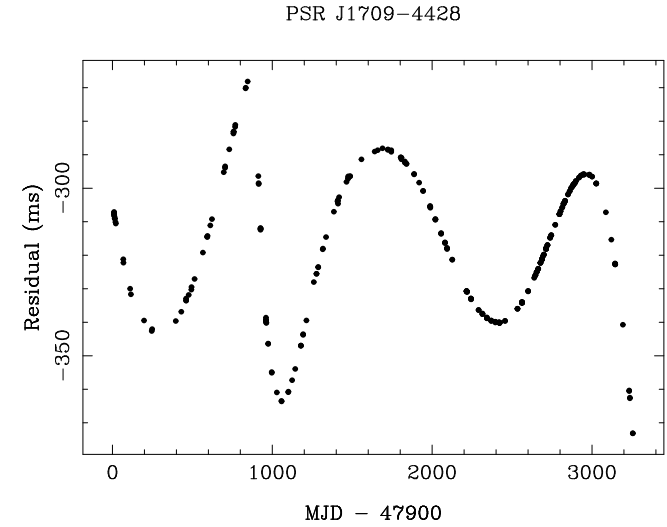


Figure 11. Post-fit timing residuals for a fit to the entire data set for PSR J1709–4428, including the glitch at MJD 48778

age, $\sim 80,000$ years. D’Alessandro & McCulloch (1997) observed this pulsar at Mt Pleasant Observatory in Tasmania from 1987 to 1994 and detected a relatively large glitch at MJD 49387.68 (1994 February 2) but found no evidence for any recovery in 10 months of observations after the glitch. The Parkes observations extend to the end of 1998 (Fig. 12) and show a clear recovery from this glitch which is roughly exponential. They also reveal a second smaller glitch in 1997 September which has a similar recovery.

Table 2 gives an improved position and DM for this pulsar. The position was determined from data between the two glitches by fitting for the position and five frequency-derivative terms to absorb the period irregularities. The DM was determined by fitting to data in the MJD range 49400 to 49900 where there were observations around 430 MHz as well as around 1400 MHz. This value is significantly different from the best previously published value ($121.9 \pm 0.1 \text{ cm}^{-3} \text{ pc}$; McCulloch et al. 1973), most probably reflecting a changing line-of-sight path through the interstellar medium. The average rate of DM change over the 24 years is $\sim 0.6 \text{ cm}^{-3} \text{ pc y}^{-1}$. DM changes have been observed in other pul-

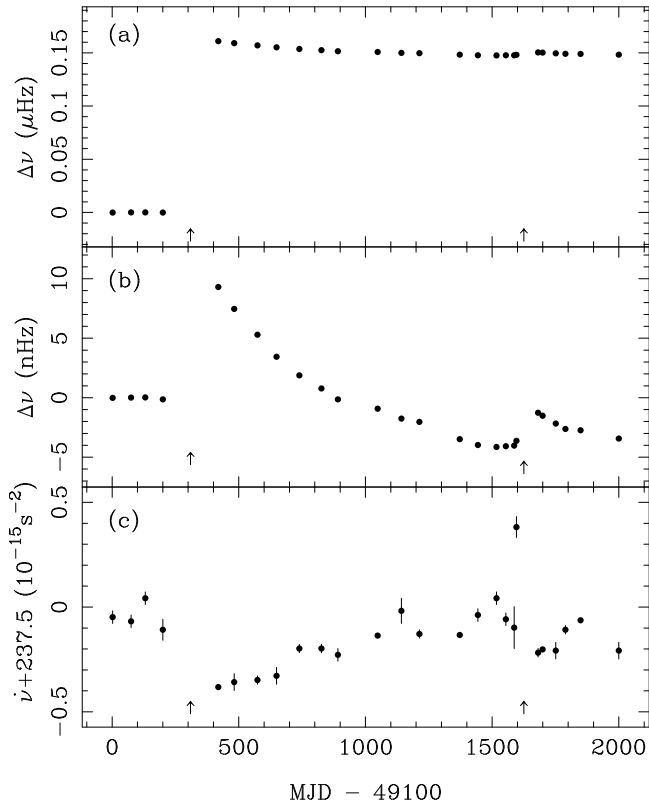


Figure 12. Glitches of PSR J1731–4744: variations of (a) frequency residual $\Delta\nu$ relative to the pre-glitch solution, (b) an expanded plot of $\Delta\nu$ where the mean residual in the inter-glitch interval has been removed from the following data, and (c) the variations of $\dot{\nu}$.

sars, notably the Crab (Isaacman & Rankin 1977) and Vela (Hamilton, Hall & Costa 1985) pulsars. The average rate of change of DM for PSR J1731–4744 is comparable to that observed for the Vela pulsar and larger than that for the Crab pulsar. The large changes observed for these two pulsars are attributed to ionised gas within the associated supernova remnant, but PSR J1731–4744 has no associated supernova remnant.

Fits to the inter-glitch intervals are given in Table 3. These fits represent the data reasonably well, except that there is a significant quartic term in the residuals for the middle interval. This is mostly due to the period irregularities which are evident in Fig. 12.

Table 4 gives parameters for the two glitches. The fitted parameters were determined by a simultaneous fit to both glitches. As mentioned above, a recovery after both glitches is clearly seen in Fig. 12, and these are well fitted by the exponential model. For the first glitch, about 8 per cent of the glitch is recovered with a time constant of about 260 days. This implies a fractional increment in $\dot{\nu}$ at the time of the glitch of 2.25×10^{-3} . The glitch parameters are in reasonable agreement with those quoted by D’Alessandro & McCulloch (1997); the differences of a few times the combined uncertainties could result from the different models used for the extrapolation to the time of the glitch. The data span following the second glitch is too short to permit solving for the

time constant, so 250 days was assumed, giving a Q value of about 25 per cent.

3.9 PSR J1801–2304, PSR B1758–23

This pulsar was detected in a search for short-period pulsars associated with supernova remnants (Manchester, D’Amico & Tuohy 1985). Despite its relatively long period of 415 ms, this pulsar has a short characteristic age (58 kyr). It lies close to the supernova remnant W28, but its association with the remnant remains controversial (Kaspi et al. 1993; Frail, Kulkarni & Vasisht 1993). It has the highest known dispersion measure ($1074 \text{ cm}^{-3} \text{ pc}$) and even at 1.4 GHz the profile is very scattered, reducing the precision of pulse timing observations at this and lower frequencies. Furthermore, the pulsar lies very close to the ecliptic plane and suffers frequent glitches, so that the pulsar position is not well determined by pulse timing; the position quoted in Table 2 and used for the timing analyses is from the VLA observations of Frail et al. (1993).

Four glitches in this pulsar occurring between 1986 and the end of 1994 were reported by Kaspi et al. (1993) and Shemar & Lyne (1996). In this paper, we present data on the last two of these glitches and two further glitches, both of relatively small amplitude, occurring in 1995 and 1996 respectively. Fig. 13 shows the variations in pulse frequency and frequency derivative around these four glitches relative to the pre-glitch solution given by Shemar & Lyne (1996) for the MJD 48454 glitch. This pre-glitch solution was adopted because that given in Table 3 is based on a data span of only 120 days and has a significantly different value of $\dot{\nu}$ from the other fits, probably as a result of intrinsic period irregularities. Fits to the inter-glitch intervals given in Table 3 have relatively large residuals because of these irregularities. Only the fit to the data following the fourth glitch required a $\ddot{\nu}$ term, indicating a significant relaxation following the glitch.

Parameters for the four glitches are given in Table 4, both from extrapolation of the polynomial fits given in Table 3 and from a simultaneous fit to the TOA data across all four glitches. Values of $\Delta\nu/\nu$ and $\Delta\dot{\nu}/\dot{\nu}$ for the first two jumps have smaller uncertainties but are consistent with the values given by Shemar & Lyne (1992). For the first three jumps the glitch epoch is determined from the requirement of phase continuity over the glitch; for the fourth glitch the data gap is too large for an unambiguous determination of the glitch epoch. Consistent with the observation of a significant $\ddot{\nu}$ term, post-fit residuals were significantly reduced by allowing an exponential relaxation following the fourth jump. However, the presence of period irregularities made fitting for the decay time impossible; the value of 100 days was found by trial to give the best representation of the data.

3.10 PSR J1801–2451, PSR B1757–24

PSR J1801–2451 is a young pulsar ($\tau_c \sim 15,000 \text{ y}$) which is located at the “beak of the Duck”, in the small nebula associated with the much larger supernova remnant G5.4–1.2 (Manchester et al. 1991; Frail & Kulkarni 1991). A giant glitch in the pulse period was observed around MJD 49476 by Lyne et al. (1996). About a year of post-glitch data

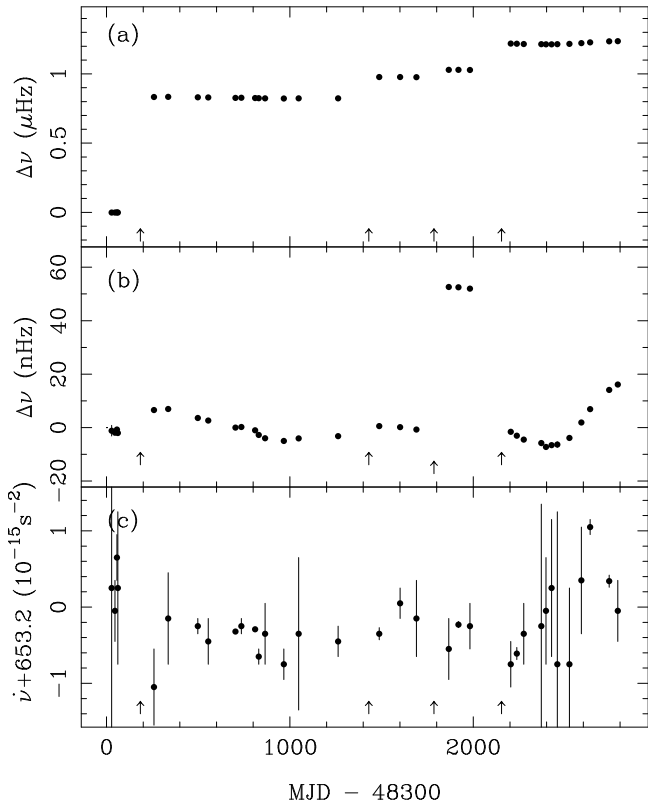


Figure 13. Glitches of PSR J1801–2304: variations of (a) frequency residual $\Delta\nu$ relative to the pre-glitch solution, (b) an expanded plot of $\Delta\nu$ where the mean residual following each glitch with a raised arrow has been removed, and (c) the variations of $\dot{\nu}$.

to MJD 49950 (1995 August) suggested a relaxation of a small fraction of the glitch ($Q \sim 0.005$) with a characteristic timescale of about 40 days.

In Fig. 14 we show observed pulse frequency variations based on Parkes data from 1992 October to 1998 December. These show the glitch observed by Lyne et al. (1996) and also a second smaller, but still large, glitch around 1997 July. Polynomial fits to the inter-glitch intervals given in Table 3 have large residuals owing to the presence of period irregularities. Extrapolation of the first two of these fits to the glitch epoch determined by Lyne et al. (1996) gives results consistent with those obtained by these authors, with $\Delta\nu_g/\nu \sim 2.0 \times 10^{-6}$. The second glitch, separated from the first by about 3.2 years, has a fractional amplitude of $\sim 1.2 \times 10^{-6}$, making it also a member of the giant glitch class.

The longer timespan of the present observations following the first glitch show that the post-glitch relaxation is best described by an exponential recovery with a timescale of several hundred days. It is likely that period irregularities were primarily responsible for the apparent quicker relaxation found by Lyne et al. (1996). There is also evidence for a similar long-timescale relaxation following the second glitch. A TEMPO fit across both glitches yielded the parameters given in Table 4, showing that, for both glitches, about 20 per cent of the glitch decayed. For the first glitch,

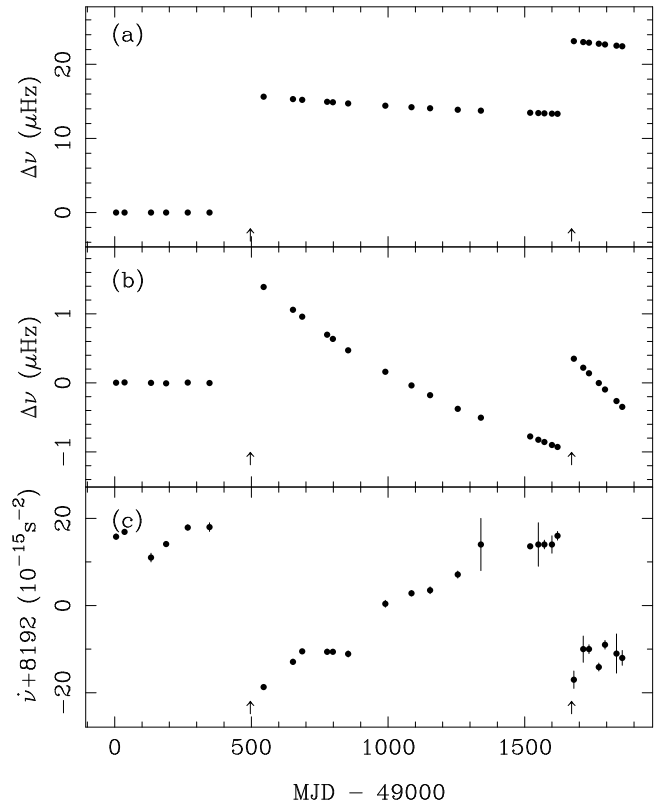


Figure 14. Glitches of PSR J1801–2451: variations of (a) frequency residual $\Delta\nu$ relative to the pre-glitch solution, (b) an expanded plot of $\Delta\nu$ where the mean residual after each glitch has been removed, and (c) the variations of $\dot{\nu}$.

the fitted timescale was 800 days. No fit of the timescale to the second glitch was possible because of the shorter data span; an assumed decay time of 600 days gave a minimum in the post-fit residuals.

3.11 PSR J1803–2137, PSR B1800–21

PSR J1803–2137 is a young pulsar ($\tau_c \sim 16,000$ y) discovered by Clifton & Lyne (1986). Lyne & Shemar (1996) observed a large glitch ($\Delta\nu_g/\nu \sim 4.1 \times 10^{-6}$) in 1990 December which showed an exponential recovery with timescale of ~ 150 d, together with an apparently linear decay in $\dot{\nu}$ indicating decay from an earlier unobserved glitch.

Our observations of this pulsar are from 1997 August to 1998 December. Fig. 15 shows that another large glitch of magnitude $\Delta\nu_g/\nu \sim 3.2 \times 10^{-6}$ occurred in 1997 November. Again, there the signature of an exponential decay following the glitch is seen. There is, however, no evidence of decay in $\dot{\nu}$ preceding the glitch (Table 3), although the data span is rather short. Table 4 gives the extrapolated and fitted parameters for the glitch. Fitting of a single exponential decay gives a relatively good fit to the post-glitch data with $Q \sim 0.13$ and $\tau_d \sim 640$ d and an rms residual of $1690 \mu\text{s}$. However, there is clear evidence in the residuals immediately after the glitch for a shorter-term decay. The glitch parameters in Table 4 are from a simultaneous fit of two ex-

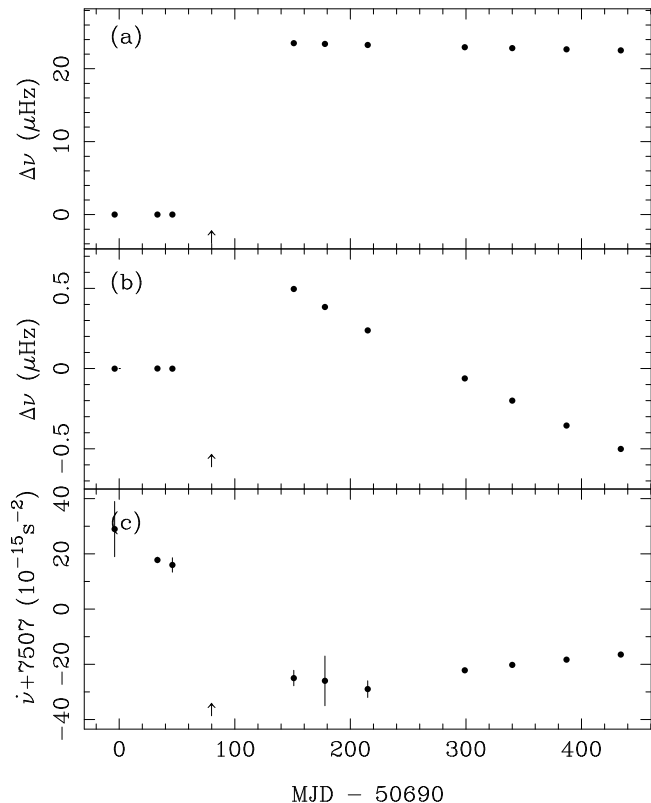


Figure 15. The 1997 December glitch of PSR J1803–2137: variations of (a) frequency residual $\Delta\nu$ relative to the pre-glitch solution, (b) an expanded plot of $\Delta\nu$ where the mean residual after the glitch has been removed, and (c) the variations of $\dot{\nu}$.

ponential decays, one with a short decay time and the other representing the longer-term decay. The final fit is extremely good, with a final rms residual of only $334 \mu\text{s}$ and the residuals dominated by random noise. Fitting of the short-term decay resulted in an increase in the estimates for Q and τ_d for the longer-term decay by about 25 per cent as shown in Table 4.

4 DISCUSSION

In this paper we have presented timing observations of 40 pulsars over various intervals up to a maximum of 8.9 years and analysed these data for improved astrometric and pulse frequency parameters and for glitch activity. In total, 30 glitches were detected in 11 pulsars, including the largest known glitch, with $\Delta\nu_g/\nu \sim 6.5 \times 10^{-6}$ in PSR J1614–5047. Twelve glitches were detected in the period of PSR J1341–6220 in a data span of 8.2 years, making this the most frequently glitching pulsar known. Evidence was found in PSR J1614–5047 for a new class of irregularity in which the pulse frequency increases markedly over a few-day interval. There appears to be an accompanying decrease in the magnitude of the frequency derivative, implying a corresponding decrease in braking torque.

Table 5 lists all known glitches, 76 in total, giving the fractional glitch amplitude $\Delta\nu_g/\nu$ and, in parentheses, the

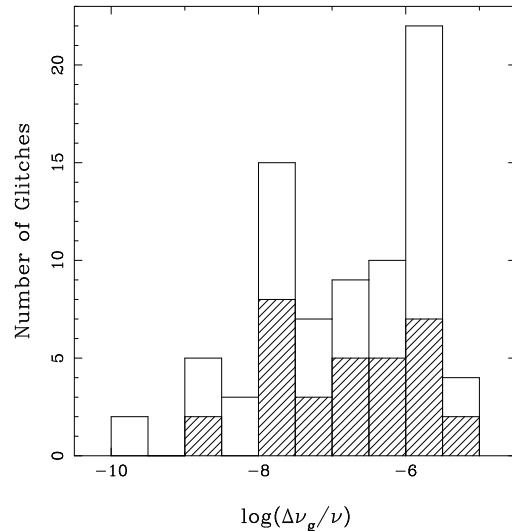


Figure 16. Histogram of fractional glitch amplitudes $\Delta\nu_g/\nu$. Values from the present study are cross-hatched.

approximate MJD of the glitch. Fig. 16 shows a histogram of fractional glitch amplitudes. Largely because of the Vela pulsar, the most common glitches are large, with $\Delta\nu_g/\nu$ in the range $1-3 \times 10^{-6}$. In most other pulsars, smaller glitches with fractional amplitude down to 10^{-8} are more common. Glitches with size smaller than 10^{-9} are difficult to identify, especially in noisy pulsars, and the sample is certainly incomplete at this level. However, there does appear to be a reduced rate of occurrence of glitches with $\Delta\nu_g/\nu < 10^{-8}$.

In most models for the glitch phenomenon, the sudden spin-up is triggered by the release of stress built up as a result of the steady spin down of the pulsar. For the original star-quake model (Baym et al. 1969), the equilibrium shape of the star becomes less oblate as the star spins down. At some point, the crust cracks and relaxes to (or toward) the new equilibrium shape, reducing its moment of inertia and hence spinning it up. However, this model fails to account for frequent giant glitches, as seen, for example, in the Vela pulsar, as the rate of change of oblateness is too slow. In models based on unpinning of internal superfluid vortices (Alpar, Cheng & Pines 1989; Ruderman, Zhu & Chen 1998), the stresses on the pinned vortices build up as the crust slows down until finally some fraction of them unpin and then repin at a larger radius, resulting in a transfer of angular momentum to the crust.

In these models, one expects some relation between the size of the glitch and the length of time that the pulsar has been slowing down since the previous glitch or the integrated change in spin rate since the last glitch. Fig. 17(a) shows glitch fractional amplitudes plotted against the length of the preceding inter-glitch interval (Δt_g), and in Fig. 17(b) against the change in spin frequency since the previous glitch ($|\dot{\nu}|\Delta t_g$). These figures show that, contrary to expectations, there is no general relation between fractional glitch amplitude and either the time since the previous glitch or the total change in spin frequency since the previous glitch. For the Vela pulsar (marked with a \star in the Figure), the smaller glitches do tend to have shorter preceding intervals and all but one of the giant glitches have preceding inter-glitch inter-

Table 5. Summary of all known glitches

PSR J	PSR B	N_g	$\Delta\nu_g/\nu$ (10^{-9})	References
0358+5413	0355+54	2	5.6(46079), 4368(46470)	1
0528+2200	0525+21	2	1.2(42057), 0.3(43810)	2,3
0534+2200	0531+21	5	9.5(40494), 37.2(42447), 9.2(46664), 85.0(47767), 4.7(48945)	4,5
0835-4510	0833-45	14	2336(40280), 2045(41192), 12(41312), 1985(42683), 3060(43690), 1137(44889), 2049(45192), 1601(46257), 1805(47520), 2715(48457), 5.6(48550), 861(49559), 198(49591), 2150(50369)	6,7,8,9,10
1048-5832	1046-58	3	19(48944), 3000(49034), 769(50788)	10
1105-6107		2	279.7(50417), 2.1(50610)	10
1123-6259		1	749.31(49705)	10
1328-4357	1325-43	1	116(43590)	11
1341-6220	1338-62	12	1509(47989), 22.5(48453), 996(48645), 13.2(49134), 146(49363), 37(49523), 15(49766), 31(49904), 1648(50008), 29.9(50321), 23.4(50528), 707.5(50683)	3, 10, 12
1509+5531	1508+55	1	0.22(41675)	13
1539-5626	1535-56	1	2790.4(48165)	3, 14
1614-5047	1610-50	1	6460(49802)	10
1644-4559	1641-45	3	191(43390), 803.9(46453), 1.9(47589)	15, 16, 17
1709-4428	1706-44	1	2028(48778)	3, 10, 14
1730-3350	1727-33	1	3070(47990)	3, 14
1731-4744	1727-47	2	139.2(49387), 3.1(50703)	10
1739-2903	1736-29	1	2.9(46956)	3, 14
1740-3015	1737-30	9	427(46991), 31(47281), 35(47458), 601.9(47670) 642(48186), 48(48218), 15.7(48431), 10.0(49046), 169.6(49239)	3
1801-2304	1758-23	6	217(46907), 231.9(47855), 351(48454), 60.8(49701), 17.0(50050), 87(50412)	3, 10, 18
1801-2451	1757-24	2	1988(49476), 1248(50651)	10, 19
1803-2137	1800-21	2	4073(48245), 3185(50765)	3, 10
1826-1334	1823-13	2	2718(46507), 3049(49014)	3
1833-0827	1830-08	1	1865.9(48041)	3
1901+0716	1859+07	1	30(46859)	3
2225+6535	2224+65	1	1707(43072)	3, 20

1. Lyne (1987) 2. Downs (1982) 3. Shemar & Lyne (1996) 4. Lohsen (1975) 5. Lyne et al. (1993) 6. Cordes et al. (1988) 7. McCulloch et al. (1987) 8. McCulloch et al. (1990) 9. Flanagan (1995a) 10. This paper 11. Newton et al. (1981) 12. Kaspi et al. (1992) 13. Manchester et al.(1974) 14. Johnston et al. (1995) 15. Manchester et al.(1978) 16. Flanagan (1993) 17. Flanagan (1995b) 18. Kaspi et al. (1993) 19. Lyne et al. (1996a) 20. Lyne (1996)

vals of about 1000 days. However, for PSR J1341-6220 there is if anything an inverse relationship, with larger glitches occurring after shorter intervals. For PSR J1740-3015 there is no relationship between glitch size and preceding interval. Fig. 17(b) shows that similar relationships for individual pulsars hold when glitch size is plotted against accumulated spin-down since the last glitch. The three points to the right on this plot are for the Crab pulsar; these too show an inverse relationship.

Alternatively, if a small glitch results from a release of only part of the built-up stress, one might expect another glitch to occur soon after, when the breaking strain is again reached. Conversely, if a large glitch releases all or most of the stress, a long time would be required for it to build up again. This suggests a correlation between glitch size and time to the *next* glitch. Fig. 18 shows glitch size plotted against duration of the following inter-glitch interval and accumulated spin-down in that period. No such correlation is observed for the Vela pulsar, where the small glitches are followed by relatively long intervals, but a weak positive correlation is seen for PSR J1341-6220 and PSR J1740-3015. Excepting the Crab pulsar, other pulsars (marked with a dot) have a good correlation between glitch size and accumulated spin-down frequency following the glitch.

These results suggest that the triggering of glitches is

a local phenomenon, not dependent on global stresses. This lends some support to the ideas of Ruderman et al. (1998) in which migration of magnetic flux tubes determines the stresses on the pinned vortices. This model is also supported by the observations of the “slow” glitches and subsequent decrease in slow-down rate in PSR J1614-5047.

McKenna & Lyne (1990) introduced the glitch activity parameter, A_g , defined to be the accumulated pulse frequency change $\Delta\nu_g$ due to glitches divided by the observation data span. It therefore has the same units as $\dot{\nu}$ and represents the portion of $\dot{\nu}$ which is overcome by glitches. This is typically small; the largest known value of A_g , for the Vela pulsar, is $\sim 2.5 \times 10^{-13} \text{ s}^{-2}$, only about 2 per cent of its spin-down rate $\dot{\nu} \sim 1.6 \times 10^{-11} \text{ s}^{-2}$. Fig. 19(a) shows activity parameter plotted against characteristic age, τ_c for most of the pulsars with extensive timing data. As noted by McKenna & Lyne (1990), there is a clear peak in activity for pulsars with ages between 2,000 and 20,000 years.

However, there is a substantial group of young pulsars with low glitch activity; these so far have had no observed glitch and are represented by upper limits in Fig. 19(a) corresponding to a single glitch of fractional size 10^{-9} . These eight pulsars have a mean data span of more than six years and so, at the least, they are infrequent glitchers. A single glitch of amplitude $\sim 10^{-6}$ would raise them into the same

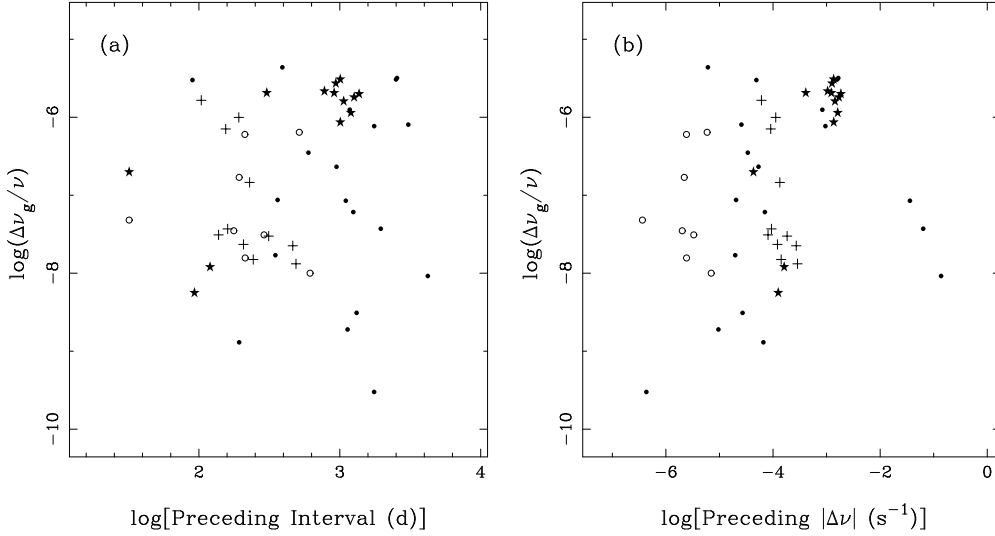


Figure 17. (a) Fractional glitch amplitude $\Delta\nu_g/\nu$ versus length of the preceding inter-glitch interval. (b) Fractional glitch amplitude $\Delta\nu_g/\nu$ versus accumulated spin-down frequency during the preceding inter-glitch interval. In both plots, points for the Vela pulsar (PSR J0835–4510) are marked with a \star , those for PSR J1341–6220 are marked with $+$, and those for PSR J1740–3015 (PSR B1737–30) are marked with \circ .

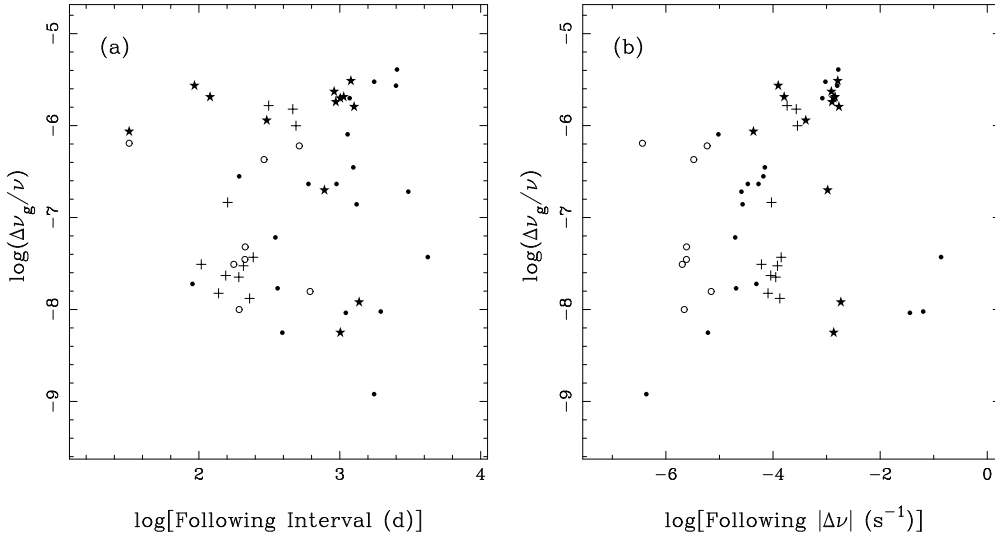


Figure 18. (a) Fractional glitch amplitude $\Delta\nu_g/\nu$ versus length of the following inter-glitch interval. (b) Fractional glitch amplitude $\Delta\nu_g/\nu$ versus accumulated spin-down frequency during the following inter-glitch interval. In both plots, points for the Vela pulsar (PSR J0835–4510) are marked with a \star , those for PSR J1341–6220 are marked with $+$, and those for PSR J1740–3015 (PSR B1737–30) are marked with \circ .

region as the other young pulsars. The dashed line corresponds to a uniform accumulated $\dot{\nu}$ over the characteristic spin-down time. This is approximately true for pulsars with age of less than or about 10^6 years, but older pulsars clearly have less glitch activity than predicted by this rule.

In Fig. 19(b) the activity parameter is plotted against the absolute value of $\dot{\nu}$. Some theoretical models for glitches (e.g. Ruderman, Zhu & Chen, 1998) predict that the ratio of the effective spin-up rate due to glitches to the spin-down rate is proportional to the ratio of the moment of inertia of the crustal superfluid to the total moment of inertia of the neutron star. A constant ratio corresponds to a line of slope -1 in Fig. 19(b). For the younger pulsars, except PSR B0531+21 (Crab) and PSR B1509–58, the points cor-

respond to a fraction of 1–2 per cent (cf. Lyne et al. 1999). Pulsars with spin-down rates less than about 10^{-14} s^{-1} have a significantly smaller fraction of their spindown recovered by glitches.

When a significant post-glitch decay is observed, it is generally well described by the exponential relation given in Equation 2. In Fig. 20(a) the fraction of the glitch which decays, $Q = \Delta\nu_d/\Delta\nu_g$ is plotted against characteristic age. With one exception, PSR B0525+21, old pulsars tend to have low values of Q . Younger pulsars can have larger Q , but many glitches in young pulsars have little or no decay.

Fig. 20(b) is a plot of glitch decay timescale versus pulsar characteristic age. This shows that, apart from the Crab pulsar (the three points in the lower left of the figure) in

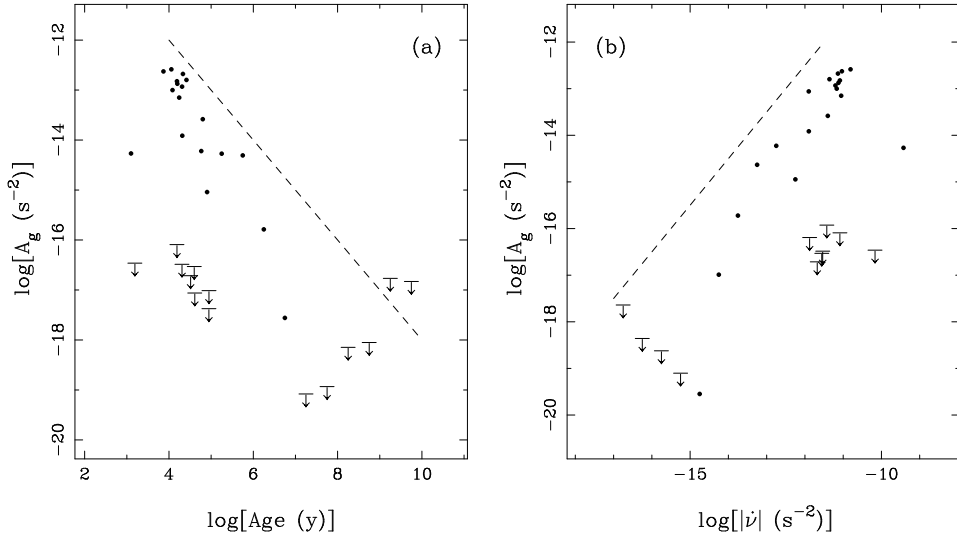


Figure 19. (a) Plot of glitch activity parameter, A_g , versus characteristic age τ_c . Pulsars with $\tau_c < 10^5$ yr are plotted individually, whereas those with greater $\tau_c > 10^5$ yr are mean values in half-decade bins. Where no glitch was observed, the upper limit is based on a single glitch of fractional amplitude 10^{-9} over the total data span, summed over all pulsars in the case of binned data. Upper limits are higher for the very old pulsars simply because there are fewer of them known and the total accumulated data span is less. The dashed line has a slope of -1.0 . (b) A similar plot with the absolute value of the spindown rate $\dot{\nu}$ as abscissa. Points with $|\dot{\nu}| > 10^{-12}$ are plotted separately while those with $|\dot{\nu}|$ less than this value are binned.

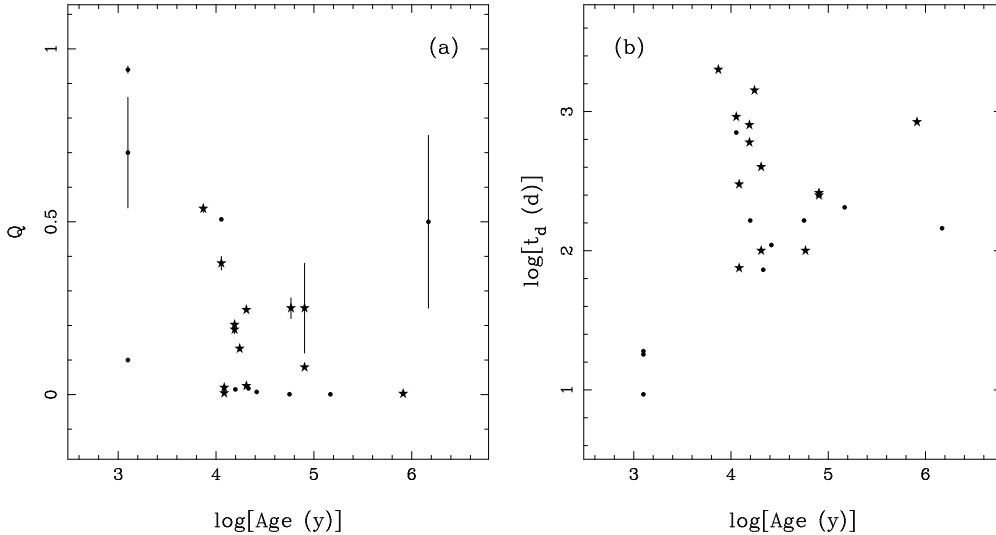


Figure 20. (a) Plot of Q , the fraction of $\Delta\nu_g$ which decays, versus characteristic age. (b) Plot of glitch decay timescale versus characteristic age. Results from this work are marked with a \star .

which the decay timescale is very short, there is no relation between decay timescale and pulsar age. We emphasise that this result applies to the longest decay timescale present. This may indicate the unreliability of characteristic age as an indicator of true age and hence internal temperature, or it may indicate that decay time, at least for pulsars with age greater than a few thousand years, is dependent on other properties, for example, the core magnetic field.

These observations have demonstrated the great diversity of glitch properties. Glitch activity is clearly greatest in pulsars with ages of between a few times 10^3 and 10^5 years. The Crab pulsar has distinctly different glitch properties from those of the middle-aged pulsars, and other pul-

sars of similar age show no glitches at all. Apart from these clear trends, glitch properties vary greatly, both for successive glitches from a given pulsar and across different pulsars, with few systematic trends. These properties suggest that the glitch phenomenon, both the event and the following response, depend on quasi-random processes occurring in the pulsar, rather than global properties such as slow-down rate or age. Crustal processes driven by magnetic field evolution as proposed by Ruderman et al. (1998) seem more consistent with this than the vortex creep models of Alpar et al. (1989).

ACKNOWLEDGEMENTS

We thank the many colleagues who have helped with observing and software development over the course of this project, and the staff of Parkes Observatory for their always cheerful assistance. In particular, we thank John Sarkissian for doing much of the observing during 1998, and Matthew Britton, Stuart Anderson and John Yamasaki for help with correlator hardware and software development. NW thanks the National Nature Science Foundation (NNSF) of China for their support of this work and VMK acknowledges support from an Alfred P. Sloan Research Fellowship. The Parkes radio telescope is part of the Australia Telescope which is funded by the Commonwealth of Australia for operation as a National Facility managed by CSIRO.

REFERENCES

- Alpar M. A., Cheng K. S., Pines D., 1989, *ApJ*, 346, 823
Alpar M. A., Cheng K. S., Pines D., Shaham J., 1988, *MNRAS*, 233, 25
Alpar M. A., Chau H. F., Cheng K. S., Pines D., 1993, *ApJ*, 409, 345
Anderson P. W., Itoh N., 1975, *Nat*, 256, 25
Arzoumanian Z., Nice D. J., Taylor J. H., Thorsett S. E., 1994, *ApJ*, 422, 671
Baym G., Pethick C., Pines D., Ruderman M., 1969, *Nat*, 224, 872
Becker W., Brazier K. T. S., Trümper J., 1995, *AA*, 298, 528
Clifton T. R., Lyne A. G., 1986, *Nat*, 320, 43
Clifton T. R., Lyne A. G., Jones A. W., McKenna J., Ashworth M., 1992, *MNRAS*, 254, 177
Cordes J. M., Downs G. S., 1985, *ApJS*, 59, 343
Cordes J. M., Downs G. S., Krause-Polstorff J., 1988, *ApJ*, 330, 847
D'Alessandro F., McCulloch P. M., 1997, *MNRAS*, 292, 879
D'Amico N., Stappers B. W., Bailes M., Martin C. E., Bell J. F., Lyne A. G., Manchester R. N., 1998, *MNRAS*, 297, 28
Downs G. S., 1982, *ApJ*, 257, L67
Flanagan C. S., 1990, *Nat*, 345, 416
Flanagan C. S., 1993, *MNRAS*, 260, 643
Flanagan C. S., 1995a, in Alpar A., Kiziloğlu Ü., van Paradis J., eds, *The Lives of Neutron Stars (NATO ASI Series)*. Kluwer, Dordrecht, p. 181
Flanagan C., 1995b, *Ap&SS*, 230, 359
Flanagan C., 1996, *IAU Circ. No.* 6491
Frail D. A., Kulkarni S. R., 1991, *Nat*, 352, 785
Frail D. A., Scharringhausen B. R., 1997, *ApJ*, 480, 364, (FS97)
Frail D. A., Kulkarni S. R., Vasisht G., 1993, *Nat*, 365, 136
Hamilton P. A., Hall P. J., Costa M. E., 1985, *MNRAS*, 214, 5P
Isaacman R., Rankin J. M., 1977, *ApJ*, 214, 214
Johnston S., Lyne A. G., Manchester R. N., Kniffen D. A., D'Amico N., Lim J., Ashworth M., 1992, *MNRAS*, 255, 401
Johnston S., Manchester R. N., Lyne A. G., Kaspi V. M., D'Amico N., 1995, *AA*, 293, 795
Kaspi V. M., Manchester R. N., Johnston S., Lyne A. G., D'Amico N., 1992, *ApJ*, 399, L155
Kaspi V. M., Lyne A. G., Manchester R. N., Johnston S., D'Amico N., Shemar S. L., 1993, *ApJ*, 409, L57
Kaspi V. M., Manchester R. N., Siegman B., Johnston S., Lyne A. G., 1994, *ApJ*, 422, L83
Kaspi V. M., Bailes M., Manchester R. N., Stappers B. W., Bell J. F., 1996, *Nat*, 381, 584
Kaspi V. M., Bailes M., Manchester R. N., Stappers B. W., Sandhu J. S., Navarro J., D'Amico N., 1997, *ApJ*, 485, 820
Kaspi V. M., Lackey J. R., Mattox J., Manchester R. N., Bailes M., Pace R. 2000. *astro-ph/9906373*
Kaspi V. M., Taylor J. H., Ryba M., 1994, *ApJ*, 428, 713
Kifune T. et al., 1995, *apj*, 438, L91
Lohsen E., 1975, *Nat*, 258, 688
Lyne A. G., 1987, *Nat*, 326, 569
Lyne A. G., 1996, in Johnston S., Walker M. A., Bailes M., eds, *Pulsars: Problems and Progress*, IAU Colloquium 160. Astronomical Society of the Pacific, San Francisco, p. 73
Lyne A. G., 1999, in Arzoumanian Z., van der Hooft F., van den Heuvel E. P. J., eds, *Pulsar Timing, General Relativity, and the Internal Structure of Neutron Stars*. North Holland, Amsterdam, p. 141
Lyne A. G., Pritchard R. S., Smith F. G., 1993, *MNRAS*, 265, 1003
Lyne A. G., Kaspi V. M., Bailes M., Manchester R. N., Taylor H., Arzoumanian Z., 1996a, *MNRAS*, 281, L14
Lyne A. G., Pritchard R. S., Smith F. G., Camilo F., 1996b, *Nat*, 381, 497
Lyne A. G., Shemar S. L., Smith F. G., 1999, *MNRAS*, Submitted
Manchester R. N., Taylor J. H., 1974, *ApJ*, 191, L63
Manchester R. N., D'Amico N., Tuohy I. R., 1985, *MNRAS*, 212, 975
Manchester R. N., Newton L. M., Goss W. M., Hamilton P. A., 1978, *MNRAS*, 184, 35P
Manchester R. N., Kaspi V. M., Johnston S., Lyne A. G., D'Amico N., 1991, *MNRAS*, 253, 7P
Manchester R. N. et al., 1996, *MNRAS*, 279, 1235
McAdam W. B., Osborne J. L., Parkinson M. L., 1993, *Nat*, 361, 516
McCulloch P. M., Komesaroff M. M., Ables J. G., Hamilton P. A., Rankin J. M., 1973, *Astrophys. Lett.*, 14, 169
McCulloch P. M., Klekociuk A. R., Hamilton P. A., Royle G. W. R., 1987, *Aust. J. Phys.*, 40, 725
McCulloch P. M., Hamilton P. A., McConnell D., King E. A., 1990, *Nat*, 346, 822
McKenna J., Lyne A. G., 1990, *Nat*, 343, 349
Navarro J., 1994, PhD thesis, California Institute of Technology
Newton L. M., Manchester R. N., Cooke D. J., 1981, *MNRAS*, 194, 841
Nicastro L., Johnston S., Koribalski B., 1996, *AA*, 306, 49
Ruderman M., 1991, *ApJ*, 382, 587
Ruderman M., Zhu T., Chen K., 1998, *ApJ*, 492, 267
Sandhu J. S., Bailes M., Manchester R. N., Navarro J., Kulkarni S. R., Anderson S. B., 1997, *ApJ*, 478, L95
Shemar S. L., Lyne A. G., 1996, *MNRAS*, 282, 677
Standish E. M., 1990, *AA*, 233, 252
Stappers B. W., Gaensler B. M., Johnston S., 1999, *MNRAS*, (SGJ99)
Taylor J. H., Manchester R. N., Lyne A. G., 1993, *ApJS*, 88, 529
Thompson D. J. et al., 1992, *Nat*, 359, 615
Thompson D. J. et al., 1996, *ApJ*, 465, 385